LA-13725-MS

Approved for public release;
distribution is unlimited.

Radiolysis of Salts and Long-Term Storage Issues for Both Pure and Impure PuO_2 Materials in Plutonium Storage Containers

Los Alamos
NATIONAL LABORATORY

Los Alamos National Laboratory is operated by the University of California for the United States Department of Energy under contract W-7405-ENG-36.

Edited by Linda K. Wood, Group CIC-1

An Affirmative Action/Equal Opportunity Employer

LA-13725-MS

Issued: May 2000

Radiolysis of Salts and Long-Term Storage Issues for Both Pure and Impure PuO_2 Materials in Plutonium Storage Containers

Lav Tandon

Los Alamos
NATIONAL LABORATORY
Los Alamos, New Mexico 87545

Table of Contents

Radiolysis of Salts and Long-Term Storage Issues for Both Pure and Impure PuO_2 Materials in Plutonium Storage Containers

by

Lav Tandon

ABSTRACT

The Material Identification and Surveillance (MIS) project sponsored a literature search on the effects of radiation on salts, with focus on alkali chlorides. The goal of the survey was to provide a basis for estimating the magnitude of alpha (α) radiation effects on alkali chlorides that can accompany plutonium oxide (PuO_2) into storage. Chloride radiolysis can yield potentially corrosive gases in plutonium storage containers that can adversely affect long-term stability. This literature search was primarily done to provide a tutorial on this topic, especially for personnel with nonradiation chemistry backgrounds.

Phase I of the report provides an overview on the following topics: (1) fundamental theory on interaction of radiation with matter in liquid water, brine solutions, and salts; (2) summary of selected literature reports on radiolysis of salts and other matrices; (3) radiation-induced thermal effects in salts; and (4) plutonium dioxides.

Phase II of this report deals with the core issues pertaining to radiolysis of chloride salts in the storage environments.

To predict the amounts of the corrosive chloride species formed in the DOE-STD-3013 containers as a result of radiation damage to the salts, one needs to know either the experimental or the theoretical G values. However, studies on the effects of α radiation are relatively few when compared to the extensive literature on effects of more penetrating beta (β) particles, x-rays, or gamma (γ)-ray radiation. It is important to consider the various transient species and the reaction scenarios. Information based on several years of practical experience with these materials at Los Alamos National Laboratory (LANL) and other DOE sites is discussed. Results from headspace gas analysis of actual containers received from Hanford Site are also discussed.

Phase I

Literature Search on the Radiolytic Effects of Ionizing Radiation in High-Salt Environments: Application to Storage of Chlorides that Accompany Plutonium Oxide

ABSTRACT

The Material Identification and Surveillance (MIS) project sponsored a literature search on the effects of radiation on salts, with focus on alkali chlorides. The goal of the survey was to provide a basis for estimating the magnitude of alpha (α) radiation effects on alkali chlorides that can accompany plutonium oxide (PuO_2) into storage. Chloride radiolysis can yield potentially corrosive gases in plutonium storage containers that can adversely affect long-term stability. This literature search was primarily done to provide a tutorial on this topic, especially for personnel with nonradiation chemistry backgrounds.

This section (Phase I) of the report provides an overview on the following topics:

- fundamental theory on interaction of radiation with matter in
  - liquid water,
  - brine solutions, and
  - salts;
- summary of selected literature reports on radiolysis of
  - salts and
  - other matrices;
- radiation-induced thermal effects in salts; and
- plutonium dioxides.

Theory

Interaction of Radiation with Solid or Liquid Matter

Exposing matter to ionization radiation causes chemical changes that result from the formation of ions, excited molecules, and free radicals along the trajectories of ionizing radiation. The amount of chemical change in matter depends on both the total quantity of radiation energy available and the rate at which the energy is deposited. The available radiation energy determines the number of reactive transient intermediates produced, whereas the energy deposition rate yields the local concentration of these intermediates along the particle tracks (Johnson 1970, Spinks and Wood 1990).

Linear energy transfer (LET) is a measure of the rate of energy deposition along the track. Alpha particles have limited range and higher LET than gamma (γ) rays or electrons, and have four times the LET of the protons of same energy (Turner 1986). High LET in solids also produces high local temperatures, which cause a local expansion (or even melting) along the tracks of ionizing particles (Johnson 1970).

The kinds of species formed tend to be the same in a particular material, regardless of the type or energy of the radiation responsible (Bjergbakke et al. 1989, Spinks and Wood 1990, Turner 1986). However, because radiation of different types and energy have different LETs, the tracks or spurs may either be densely or sparsely populated with active species, yielding differences in the quantity of the chemical products (Levy and Kierstead 1984).

Alpha decay of radionuclides produces both a high-energy α particle (~ 4–6 MeV) and a recoil nucleus (~0.1 MeV). Nearly all the energy of the recoil nucleus is lost through elastic collisions that produce several thousand atomic displacements. Most of the energy in an α particle is dissipated in the ionization processes, but sufficient energy is lost through elastic collisions to produce several hundred displacements (Weber and Ewing 1997). Every plutonium atom in any matrix with a similar weapons-grade isotopic composition will be displaced one time in a 10-year period. For electrons, x-rays, and gamma (γ) rays, the number of atomic displacements produced during energy loss is insignificant compared to α particles (Johnson 1970).

For the α-emitting forms in which the crystal size is small (in the 0.1–10-μm range), the α particle (with a range of ~20 μm) effectively bombards the entire solid, as well as the nonactinide-containing phases. The damage caused by the recoil nucleus, because of its short range (~0.1 μm), is confined to the phase in which the actinide is chemically incorporated (Weber et al. 1981).

In heavy particle radiation, such as protons, deuterons, and α particles, the spurs overlap and form a column of free radicals, ions, and excited species about the track. Low-LET radiation (γ rays, x-rays, or fast electrons) produces spurs at longer intervals along the tracks. Therefore, free radicals and other reactive species, as compared to α particles, are more prone to react with scavengers in cases of less densely ionizing radiation (Spinks and Wood 1990).

Scavengers for free-radicals include

- oxygen,
- nitric oxide,
- chlorine,
- hydrogen chloride,
- iodine,
- hydrogen iodide and organic iodides,
- transition metal salts (e.g., ferric chloride),
- stable free radicals (e.g., diphenylpicrylhydrazyl, [DPPH]), and
- unsaturated organic compounds.

If present at high enough concentrations (1000 mol m^{-3}), scavengers can consume radicals and other reactive species that would otherwise react within the track or spur zone. At lower concentrations, the scavengers will scrounge radicals that have only thermal energy or that have escaped from the tracks; hot radicals normally will not be scavenged (Spinks and Wood 1990).

Radiation damage includes effects on the physical properties of the crystals, such as the ionic conductivity, density, and hardness. For various nuclear waste forms, the changes in properties, such as lattice parameters, density, and stored energy of the waste (for both the actinide host and nonactinide-containing phases), saturate at a dose of 5×10^{18} α decays/cm^3 (Weber et al. 1981).

The retention of α-decay damage in solids, particularly crystalline materials, depends on the energy barrier of the solid to recrystallization. If the barrier is low, the radiation damage will anneal itself as it takes place (Wronkiewicz 1994). Radiation damage can also lead to increased leaching of the actinides in vitrified wastes (Weber et al. 1983). The number of α decays/cm^3/yr for the material with the following isotopic composition:

> ^{238}Pu, ^{239}Pu, ^{240}Pu, ^{241}Pu, ^{242}Pu, and ^{241}Am in wt % of 0.008, 94.2, 5.7, 0.11, 0.02, and 0.17 respectively, will be 1.04×10^{18} α decays/cm^3/yr.

Therefore, without taking the decay into account, the radiation damage in both PuO_2 and the salts should saturate in ~5 yr.

Radiation-chemical yields have been generally described in terms of G values, where G (X) is the number of molecules of product X formed, or of the starting material Y consumed (shown as G [–Y]), per 100 eV energy absorbed. G values for many compounds range from 1 to 10, although there are many exceptions.

Liquid Water

If the radiation damage in salts is large, they will be chemically very reactive, particularly if water or brine is present (Levy and Kierstead 1984). For the focus of this review, we will include the extensive literature on effects of radiation on water only to the extent needed for applications to solids. It should be mentioned that most of the literature reports deal with liquid water radiolysis, whereas the main concern for this project is water adsorbed on PuO_2 surface. It is believed that any layers of water after the first monolayer will behave as liquid water and, therefore, the basic principles of radiolysis of water will still be the same. The presence of liquid water (even at trace levels) plays a key role in the radiolysis reactions that accompany the interaction of radiation with matter.

The unique aspects of the radiation chemistry of liquid water include the following (Spinks and Wood 1990).

- All charged species with only thermal energy become hydrated very rapidly.
- Excitation energy is lost by a collision process very quickly; in water this is facilitated by highly hydrogen-bonded structure of the system.
- The different species that are formed are close together. Those formed with only thermal energy will be constrained to remain close together for a long time. Therefore, the diffusion in water is slow. The consequences of this slow diffusion process include the formation of a cage and of spurs and tracks that describe the inhomogeneous distribution of primary species.

The radiation chemistry of pure water is relatively well understood. The following radical, ionic, or molecular species are formed when water undergoes radiolysis:

$$H_2O \rightarrow e_{aq}^-, OH\cdot, H\cdot, H_2O_2, H_2, H^+ \quad .$$

Major reactions in the radiolysis of liquid water are as follows (Spinks and Wood 1990):

$$H_2O \rightarrow H_2O^+, e^-, H_2O^* \quad , \qquad (1)$$

$$H_2O^+ + H_2O \rightarrow H_3O^+ + OH\cdot \quad , \qquad (2)$$

$$H_2O^* \rightarrow H_2O \quad , \tag{3}$$

$$H_2O^* \rightarrow [H\cdot + OH] \rightarrow H_2O \quad , \tag{4}$$

$$e^- \rightarrow e_{aq}^- \quad , \tag{5}$$

$$e_{aq}^- + H_2O \rightarrow H\cdot + OH^- \quad , \tag{6}$$

$$2e_{aq}^- \rightarrow H_2 + 2OH^- \quad , \tag{7}$$

$$e_{aq}^- + H\cdot \rightarrow H_2 + OH^- \quad , \tag{8}$$

$$e_{aq}^- + OH\cdot \rightarrow OH^- \quad , \tag{9}$$

$$e_{aq}^- + H_3O^+ \rightarrow H_2O + H\cdot \quad , \tag{10}$$

$$2H\cdot \rightarrow H_2 \quad , \tag{11}$$

$$H\cdot + OH\cdot \rightarrow H_2O \quad , \tag{12}$$

$$2OH\cdot \rightarrow H_2O_2 \quad , \tag{13}$$

$$OH\cdot + H_2O_2 \rightarrow H_2O + HO_2 \quad , \tag{14}$$

$$HO_2 \rightarrow H_2O_2 + O_2 \quad , \tag{15}$$

$$H_3O^+ + OH^- \rightarrow 2H_2O \quad , \text{ and} \tag{16}$$

$$H_3O^+ + OH^- \leftrightarrows 2H_2O \quad . \tag{17}$$

These are the most important reactions involving primary radicals and radiolysis products. Additional reactions are known to take place but are not necessary to enable a reasonable discussion of aqueous solutions (Sullivan 1983). Competition kinetics can be applied to predict which of the competing reactions will predominate. If dissolved oxygen is present, species such as O_2^- and HO_2, also can be produced. Because the decomposition mechanism of water does not depend on the nature of radiation, the yield of each radiolysis product is directly influenced by LET, which is much greater for α particles than for γ rays.

A comparison of the G values for the radiolysis of water indicates that γ radiation produces greater concentrations of e^-_{aq}, OH, and hydrogen, whereas α yields are higher for molecular species such as HO_2, H_2O_2, H_2, and H_2O (Büppelmann et al. 1988, Wronkiewicz 1994).

These molecular species occur because the distance between the spurs for α particles is very close and the expanding spurs will overlap from the moment of formation (Samuel and Magee 1953). Such overlapping yields a denser concentration of radicals with increased probability of recombination.

A comparison of G (hydrogen) values of water using both α and γ sources also indicated a strong dependence on LET. G (hydrogen) increased by a factor of 3 to 4 from γ radiolysis to α radiolysis (Spinks and Wood 1990, Bibler 1975, Bibler 1974, Burns and Sims 1981). LET for α particles decreases with energy that is greater than 1.5 MeV. G (hydrogen) values for irradiated water and aqueous salt solutions are often controlled by a back-reaction of hydrogen with the OH· radical to form water (Gray and Simonson 1984). Hyder and others (1998) recently published a literature review pertinent to core technology research for the 94-1 Research and Development Project on recombination of water. Further studies on this subject are currently in progress at Los Alamos National Laboratory (LANL) and will be discussed in other publications.

However, the presence of impurities dissolved in water (such as Br^-, Cl^-, which act as scavengers of the OH· radical) will increase the yield of hydrogen in the gas phase (Büppelmann et al. 1988, Gray and Simonson 1984). Moreover, some researchers have suggested that the G (hydrogen) values and equilibrium concentrations of hydrogen are controlled by a back-reaction of hydrogen with the OH^- to form water (Bibler and Orebaugh 1977, Gray and Simonson 1984). This back-reaction and the resulting G (hydrogen) values were found to be three to four times higher for α radiolysis as compared to γ radiolysis. A comparison of G values for various primary products in irradiated water, after α and γ irradiation, reveal two key features.

- First, the G values for primary radiolysis products are very small for both kinds of irradiation because a host of secondary reactions have a net effect of regenerating water (Allen et al. 1952, Büppelmann et al. 1988, Gray and Simonson 1984, Van Konynenburg et al. 1996); and
- Second, the molecular species predominate for α irradiation.

Regardless of the nature of water present in the material (i.e., if it is present as either adsorbed liquid or absorbed liquid, radiolysis experiments indicate that the sorbing medium can either be inert to radiation or can transfer all the energy to the sorbed liquid. Unless experimental data demonstrate that the binding medium is radiolytically inert (e.g., vermiculite), all the radiation energy should be assumed to interact with the sorbed water (Bibler and Orebaugh 1977). LANL researchers plan a detailed review of water radiolysis in the material of interest.

Brine Solutions

Because geological salt formations are considered possible sites for radioactive waste disposal, numerous studies on the radiolysis effects of salt brines are reported in the literature. Also of interest is radiation-chemical behavior in brines, because rock salts in geological repositories generally contain a small amount of brine inclusions that are not homogeneously distributed. Over time, these inclusions may migrate toward the high-level waste container, which acts as a heat source (McClain and Bradshaw 1970). Brines will also form in geological repositories if the groundwater reaches the salt deposits.

Halide ions in aqueous solutions are inert towards e_{aq}^- and hydrogen but undergo rapid electron-transfer-type reactions with OH· to give products (Cl_2^-, Br_2^-, and I_2^-), which incorporate a second halide ion and are stoichiometrically equivalent to $X + X^-$:

$$OH\cdot + X^- \xrightarrow{X^-} X_2^- + OH^- \quad . \qquad (18)$$

In the cases of chloride and bromide, the reaction is more rapid in the presence of hydrogen ion, but with iodide it is independent of pH. Dimerization of the species formed by the above reaction produces the corresponding halogen molecule (X_2) or an ion derived from it (X_3^-),

$$2X_2^- \rightarrow X_2 + 2X^- \text{ (or } X_3^- + X^-) \quad . \qquad (19)$$

However, only low steady-state concentrations of halogen molecule are produced when halide solutions are irradiated because the back-reactions with e_{aq}^- and H_2 occur to reform halide ion (Spinks and Wood 1990).

Bjergbakke and colleagues (1989) surveyed the compounds that may form in salt brines (overwhelmingly NaCl) when the brines are exposed to an assumed dose rate of 1 Gy/s for 1000 s. Then they predicted by extrapolation the yields of various products. The concentration of hypochlorous acid remained in a steady state at a micromolar level, but the concentration of chlorine gas was below the detection limit even for NaCl concentration of 5.5 mol/L.

$$OH\cdot + Cl^- \rightarrow ClOH^- \quad . \qquad (20)$$

$ClOH^-$ is a short-lived intermediate that is also an oxidizing agent. Subsequent reactions with chloride generate the chlorine free radical Cl· and the radical-ion Cl_2^- (an oxidizing agent also). Both take part in the reactions leading to the reformation of Cl^- ion (Bjergbakke et al. 1989, Fukasawa et al. 1996). Gamma radiolysis of brines indicates that, with increasing temperature, a decrease occurs in the equilibrium pressure of hydrogen and oxygen gases. This decrease occurs because the rate of an increase of H_2/OH reaction that forms water with temperature must be greater than the rate of increase for the reaction of OH with scavenger species Cl^-, Br^-, SO_4^-, and others. (Pederson et al. 1986).

In almost all the experiments in the literature with both α and γ radiations on brine, the gas composition above the brines is approximately two parts hydrogen gas to one part oxygen gas. Gamma radiolysis of salt brines (NaCl and NaBr solutions) indicated that the gas composition was approximately 67% hydrogen and 33% oxygen (Weber et al. 1984). However, at comparable temperatures and dose rates, the equilibrium pressures for α experiments (>136 atm) are generally higher when compared to γ experiments (100 atm).

Bjergbakke and coworkers (1989) studied radiolysis of inorganic-ion aqueous solutions (particularly chloride ions) and predicted the possible reactions and rate constants. The reactions that lead to gas accumulation depend on the irradiation conditions, such as ambient temperature, total dose accumulated, and the possibility of pressure buildup. At low solute concentrations, the solute does not greatly affect the molecular yields of radiolytic products in water. However, species that react with OH or act as scavengers (such as Cl^-, Br^-) gradually lower the molecular yield of H_2O_2 and hydrogen as the concentration of the scavengers is increased (Pederson et al. 1986).

When the concentration of solute is more than a few percent by weight, it is necessary to consider the direct action of radiation on the solute (Büppelmann et al. 1988). In chloride solutions, reactions of Cl^- in tracks with primary radiolysis products become important, provided that the chloride concentration is high enough to compete with other present species.

A summary of the significant reaction processes taking place after the radiolysis of NaCl solution is discussed by Büppelmann et al. (1988). Alpha-particle irradiation of 5-M NaCl results in the formation of transitory equilibrium system of $Cl_3^-/Cl_2/HClO/ClO^-/Cl^-$. At pH <7, the formation of chlorine gas is favored. The initial effect of radiolysis of neutral saline solutions is a rapid decrease in pH to 4, followed by a gradual increase over a period of days to neutrality (Büppelmann et al. 1988). It appears that in complex brine, some synergistic interaction occurs between Cl^- and Br^- because the two generate more pressure than the sum of individual solutions. If there is any sulfate present, the synergism between Cl^- and SO_4^{2-} is quite marked. Weber and colleagues (1984) found no chlorine greater than 10 ppm gas or its derivatives in irradiated brines.

Fundamental Principles of Radiolysis in Salts

Ionizing radiation of all types can produce ionized and excited atoms in solids. In addition, heavy particles (such as protons, deuterons, α particles) can cause a significant number of atoms to be displaced from their normal position, while γ, x-ray, and electron radiation produce mainly ionization and excitation but can cause a small amount of atomic displacement (Spinks and Wood 1990).

The heavier products of any chemical dislocation produced in a solid will effectively be caged and may recombine. Ionization of lattice anions leads to neutral atom formation, diffusion, and subsequent trapping at a crystal interstitial site. Previously, such defects in solids were described in terms of point defects, Frenkel and Schottky defects, which refer to interstitial and vacancy pairs respectively (Johnson 1970).

Atom displacement processes lead to disordering of anion and cation sublattices, which, for certain material subjected to high fluence, leads to amorphization and/or phase separation (Exarhos 1982). Lighter species, such as electrons and hydrogen atoms, can migrate through the solid matrices, although an electron particularly may become trapped at certain preferred sites in the matrix. Such displacement mechanisms are believed to be responsible for generating F centers, vacancies, and interstitials after irradiation with light ions of MeV energy range (Price and Kelly 1978).

When irradiated, alkali-halide and alkaline-earth halide crystals produce absorption bands in the visible and ultraviolet regions (Billington and Crawford 1961, Chadderton 1965, Exarhos 1982, Levy 1991, Robinson and Chandratillake 1987, Spinks and Wood 1990).

The color in the visible region varies with the nature of the crystal. For example, lithium chloride gives a yellow color and cesium and potassium chlorides give blue colors. The absorption bands responsible for these colors are known as F bands, and the defects in the crystals that give rise to them are called F centers. Additional absorption bands may be generated in the ultraviolet (UV), visible (VIS), and infrared (IR) regions; these bands also are a result of the presence of impurities. For example, the absorption bands for potassium chloride include V bands (UV), R bands (VIS), F band (red-IR), and M band (IR). If traces of calcium chloride impurities are present, Z bands are also observed.

The mechanisms for the formation of various bands are as follows. The crystal is made up of a regular three-dimensional array of positive and negative ions (Fig. 1). However, holes (vacancies) may exist in the structure in which either a positive ion (Fig. 2) or a negative ion (Fig. 3) is missing. (Similar vacancies may be formed by irradiation.)

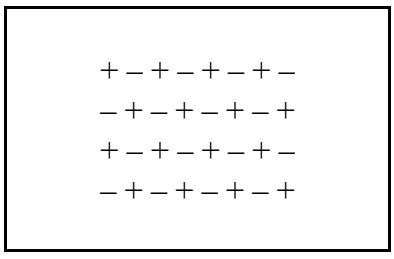

Fig. 1.* Crystal made up of a regular three-dimensional array of positive and negative ions.

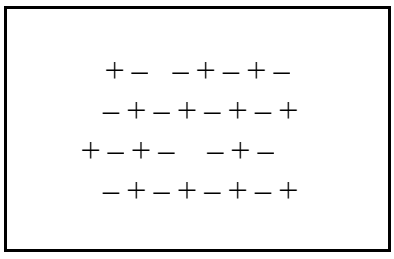

Fig. 2.* Crystal with holes (vacancies) in the structure where a positive ion is missing.

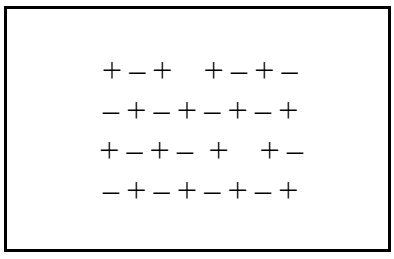

Fig. 3.* Crystal with holes (vacancies) in the structure where a negative ion is missing.

*Adapted from Spinks and Wood 1990

Irradiation can lead to electrons being ejected from some of the atoms in the crystal lattice. Whereas most of the electrons will return to their parent atom or to a similar atom that has lost an electron, some will be trapped and held in a negative ion vacancy, thus forming an F center (Fig. 4). The process is somewhat inefficient (Typically ~0.1% of radiation-produced electrons are trapped.) because the number of vacancies are low.

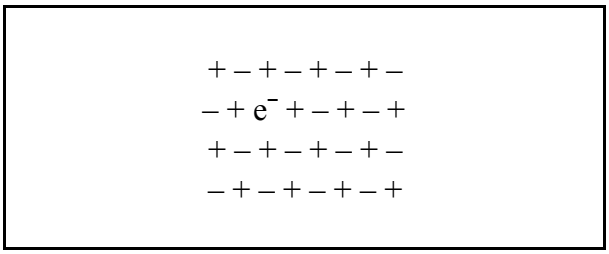

Fig. 4. Crystal with electron trapped in a negative-ion vacancy and forming an F center. (Adapted from Spinks and Wood 1990)

Formation of positive-ion vacancy and V_1 center can be illustrated for a sodium chloride crystal (Figs. 5 and 6, respectively). Positive-ion vacancy gives rise to a V_1 center.

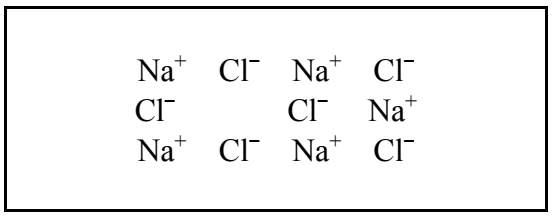

Fig. 5.* Sodium chloride crystal with formation of positive-ion vacancy.

*Adapted from Spinks and Wood 1990

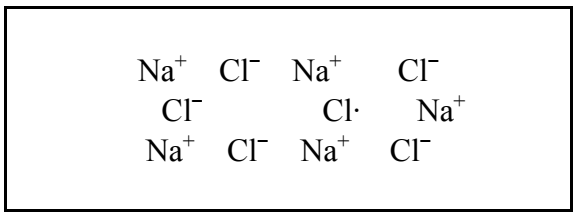

Fig. 6.* Sodium chloride crystal with formation of V_1 center.

Formation of a V_1 center follows the loss of an electron from one of the chloride ions that surrounds a positive-ion vacancy, thus giving rise to the formation of a chlorine atom. The positive-ion vacancy–chlorine atom system is stable and electrically neutral; the chlorine atom is in equilibrium with the five chloride ions surrounding the vacancy, the five electrons associated with the charge of these ions being shared between the six chlorine nuclei. In addition to arising from F, V_1 centers can arise from the displacement of atoms and ions from

their normal position in the crystal. The F centers generally aggregate to form F_2 (di-F) or M centers, F_3 or R centers, and F_4 or N centers (Wardle 1975).

In an ionic crystal such as NaCl, the ionization process is rather complex and leads to the ejection of chlorine to an interstitial position, where it associates with a neighboring Cl^- to form an H center (as shown following this paragraph). The stripped-off electron is trapped at the original place of an ejected chlorine atom and, as mentioned earlier, forms an F center (Spinks and Wood 1990).

$$Cl\cdot + Cl^- \rightarrow Cl_2^- \qquad (21)$$

These F centers are responsible for the yellow/brown color Akram and associates (1992) observed in NaCl crystals at low integrated doses. The radical –ion Cl_2^- (H-center) has a unique absorption band at 365 nm. Pretzel (1965) studied different mechanisms of radiation damage to alkali halides and suggested that Cl_2^- might be an essential intermediate to the damage process. The amount of energy transfer required for the displacement of atoms from their normal positions in an insulating crystal depends somewhat on the irradiated material, but Sonder and Sibley (1971) believe it to be in the range of 25–50 eV.

During the late stages of the irradiation of a salt specimen, a number of exposure variables are known to affect the net rate of formation of crystal defects and the number of accumulated F centers in alkali halides. These variables are the following (Levy 1991):

- temperature,
- irradiation intensity (dose rate),
- divalent cation impurities, and
- plastic strain (Clark and Crawford 1973).

Some variables also affect the initial rate of defect production by altering the fraction of electron-hole pairs that recombine at impurity sites and lose recombination energy with no defect production. Annealing of salt takes place by heating or exposing it to light and will lead to bleaching of the colors. By heating the irradiated salt to a few hundred degrees centigrade, the radiation-induced F and V_1 centers can be removed. Electrons being released from the F centers combine with the electron-deficient V_1 centers.

Impurities are also defects in a lattice. Exposure to radiation in a chemically reactive system builds up impurities. For example, irradiation of KNO_3 produces NO_2^- and oxygen, both of which are impurities and may act as trapping sites for new or additional defect centers (Johnson 1970). These defects can form color centers or be directly involved in various reactions.

Chemical changes are generally observed when the irradiated crystals are dissolved in water. Potassium chloride gives a slightly alkaline oxidizing solution, probably through the reaction of trapped electron and chlorine atoms with water (Spinks and Wood 1990),

$$e^- + H_2O \rightarrow e_{aq}^- \quad , \qquad (22)$$

$$Cl\cdot \text{ (crystal)} \rightarrow Cl^- \text{ (solution)} \quad , \qquad (23)$$

followed by

$$2Cl\cdot \rightarrow Cl_2 \text{ etc.} \quad \text{, and} \qquad (24)$$

$$2e_{aq}^- \rightarrow H_2 + 2OH^- \quad . \qquad (25)$$

When radiation-damaged salts are dissolved in water, the key issue that governs the chemical reactions is the formation of such compounds as HCl, NaOH, HOCl, OCl^-, or ClO_3^-. Consequently, the pH of the resulting solution depends on the fate of chlorine in the irradiated salt (Levy 1983, Weber et al. 1984, Weber et al. 1983). According to Pederson et al. (1986), if one assumes that no significant loss of neutral chlorine took place from the host salt after irradiation, then equal quantities of base (NaOH) and acid (HCl and HOCl) would be created upon the dissolution of the salt in water.

Summary of the Literature Reports on Salt Radiolysis

References published in the 1950s and the 1960s have been known to be unreproducible; therefore, caution needs to be exercised when one interprets results published during that time (Levy 1991). Two excellent review articles on various aspects of salt radiolysis were recently published: they are Levy (1991) and Lidiard (1998).

Low-LET Radiation Sources (electrons, β-particles, x-rays, γ-rays, and others)

More extensive decomposition of NaCl by radiolysis is indicated by the appearance of a colloidal-type absorption band. The necessary conditions for the appearance of colloidal bands have been established experimentally as follows:

- The radiation dose should be sufficiently high; and
- The crystal should contain certain activating impurities (Compton 1957, Didyk et al. 1971).

In oxygen-doped NaCl crystals, the presence of oxygen simulates the formation of excess anion vacancies that have particularly high concentration near dislocations and microblock boundaries; additional electrons appear as a result of ionization of O^{2-} ions (Tsal' and Didyk 1970). It was also shown that additional defects in the anion sublattice favor the evolution of

atomic chlorine from sodium chloride. Consequently, when a sufficiently large threshold dose of the order of magnitude 10^8–10^9 R of γ ray is absorbed, F centers coagulate to form X centers (Tsal' and Didyk 1970).

Didyk and associates (1971) determined that the presence of chlorine in the gaseous medium (after irradiation of NaCl crystals) could be detected only by a mass spectrometer with a small vacuum system in which the influence of the walls on the composition of enclosed gases is slight. This reaction with the wall of the container was likely because of the high activity of chlorine that, like oxygen, is rapidly absorbed or reacted on the walls of the vacuum system or the electrodes. Pure and Sr^{2+}-doped crystals (excess cation vacancies) indicated no evolution of Cl^+ ions immediately after opening the ampoule, after irradiation, and even after heating the system to 200°C. This lack of Cl^+ ion evolution is because the conditions for diffusion of chlorine atoms are complex in the previously mentioned systems.

Levy (1983) studied extensively the various aspects of radiation damage to different rock salt samples after they had been irradiated with 1.5 MeV-electrons. At room temperature and at low doses, only F centers (Cl^- ion vacancies) and a variety of "V region" absorption bands (mostly holes trapped on a variety of defects) were present. High doses of 10^4 to 10^5 Gy induced a blue-black color in the rock salt. This blue-black color was attributable to the presence of sodium metal colloid particles. Depending on the dose, the color can vary from blue-black to light blue to purple to grayish-white. In some cases, the formation of the color is delayed by a few months after irradiation (Levy 1983).

The formation of colloidal sodium aggregates apparently confers additional stability to radiation defects in NaCl (Burns and Williams 1955). The radiation defect formation is equivalent to energy storage in the halite. The most likely amount of total stored energy seems to be ~125 J/g NaCl at 1 mol % of radiolytically formed colloidal sodium (Gies et al. 1994).

Above 115°C and at high doses, temperature-dependent, intense colloid particles of sodium metal absorption bands are formed. Formation of F centers begins immediately after irradiation is begun and increases monotonically to a well-defined plateau, which is reached at doses of 10^4 to 10^6 Gy. Colloid formation rate increases as the dose rate increases. Apparently, a relationship exists between colloid formation and the salt impurity levels. This relationship is suppressed in regions of crystals containing ~1% calcium and sulfur. Both F center and colloid formation is strongly temperature dependent.

At fixed irradiation conditions, the F center plateau is high at 100°C and decreases monotonically to a low negligible formation at 300°C. The colloid particle formation rate is low or negligible at irradiation temperatures of 100°C to 115°C. As the radiation temperature increases to a broad maximum at 150°C to 175°C, the colloid formation decreases to a negligible level at 250°C to 300°C.

Levy (1983) found that colloid formation at high doses is proportional to t^n, where t is the irradiation time and the exponent and n is temperature and impurity dependent. For synthetic NaCl, n varies from 1.5 to 6.2. However, for natural NaCl, n varies between 1.7 to 2.2. Levy estimated that at a temperature of 150°C, where the colloidal formation rate is maximum, in 50 to 400 yrs a total dose of 10^8 Gy will convert between 0.1% and 10% of the salt to colloidal sodium metal.

On the other hand, a total dose of 2×10^8 Gy will convert 1%–50% of the salt to colloidal sodium metal (Levy and Kierstead 1984, Levy 1983, Levy et al. 1981). Rock salts from 14 sites were studied in this project. A careful examination of the data reveals that colloid formation rates vary by a factor of 10 or more between samples from different sites.

It is worth noting that the upper limit of sodium-metal colloid formation will be significantly lower at the total doses mentioned previously, except for the recrystallized rock salts from Rocanville, Saskatchewan, Canada. In fact, if this data is excluded, a maximum colloid formation of only 3.95% at 10^8 Gy and 16.7% at 2×10^8 Gy respectively is obtained. These results suggest that sometimes the origins, properties, and processing of the salts can greatly influence the extent of radiation damage observed in the salts.

Simple material balance requires one atom of chlorine to be formed for each atom of sodium that is incorporated into a colloidal sodium metal particle. The exact disposition of chlorine after radiation damage in rock salt is still uncertain. For example, it is not known for certain whether this chlorine is retained in parts of the rock salt lattice that does not contain colloid particles. When the colloid concentrations exceed 0.1%–10%, it is highly unlikely that all the chlorine that accompanies the colloid formation can be accommodated in the colloid-particle-free portion of the rock salt lattice.

Chlorine odors often have been detected when the irradiated rock salts are broken or cleaved. Jenks and Bopp (1977) attributed the source of chlorine odor to aggregates of trapped holes (Cl_2^-) on the grain boundaries, which were exposed to air by cleaving or crushing. However, because chlorine gas is highly reactive, especially in the presence of any moisture, it is important to determine whether chlorine gas was released following rock salt lattice irradiation (Levy 1983, Levy et al. 1981).

In rock salt samples from the Asse mine in Germany (which were exposed to high integrated doses), only when the integrated dose levels were of the magnitude10^7 Gy could the generation of reactive gases (such as chlorine or HCl) be observed (Palut et al. 1993). Palut and others have suggested that detecting chemically aggressive gases (such as chlorine or HCl) requires optimization of analysis and detection methods because these gases recombine very quickly with surrounding material. For smaller grain sizes of salts, the amount of released gases is generally higher.

Jockwer and Mönig (1989) studied the influence of various parameters (i.e., the total absorbed dose, the dose rate, and the temperature) on two different rock salt samples. These samples had different mineralogical compositions (primarily halite with trace amounts of anhydrite, polyhalite, kieserite, water, and gases absorbed on crystal boundaries or trapped as inclusions). The researchers subjected salts with a grain size of 1 mm to ^{60}Co γ irradiation with an integral dose of 10^9 Gy. The halite contents (on weight-% basis) in the two kinds of salt samples from the Asse mine were 72.6% and 96.6%, respectively. The water contents of these samples were 1.2% and 0.2%, respectively.

Jockwer and Mönig conducted some irradiations at various elevated temperatures to simulate the long-term exposure to high levels of radiation over an extended period that heats up the salts. Only at very high doses could corrosive gases, such as chlorine and SO_2, be detected; but their concentrations were of the order of 0.1 ppm. An important conclusion from this study by Jockwer and Mönig was that duration of radiolysis is a very important factor. Gases that are naturally present in the rock salt slowly desorbed during the irradiation in a temperature-dependent fashion. Therefore, with increasing radiolysis times, higher gas yields were observed, even though the gases might not have been direct radiolysis products. The researchers also determined that the time evolution for gas desorption at any temperature was different in irradiated samples than for samples that had not been irradiated. This finding further complicates the thermal effects (Jockwer and Mönig 1989).

Jenks and Bopp (1977) concluded that for both pure NaCl and rock salts appreciable amounts of γ energy can be stored in salt under certain exposure conditions. Their results also showed that thermally activated annealing takes place at temperatures above 150°C and negligible amounts of energy will be stored in the salt as a consequence. Below 150°C, thermally activated or radiation-induced annealing could not be shown, although researchers did not rule it out. They suggested that between 30°C and 150°C, the maximum stored energy formed in a salt (in a repository, with no annealing) would be 50 cal/g.

The γ doses used in these experiments ranged up to an amount exceeding the maximum doses (10^8 Gy) that will prevail in salt in a high-level waste repository. Jenks and Bopp (1977) also studied the loss of water from bedded salt specimens during γ irradiation. They compared the results from one of the bedded salts that contained 0.25% water (held in small brine cavities within crystals and on crystal boundaries) with pure NaCl crystals. Both salts were exposed to average γ dose rates of 10^5 Gy/h. The results indicated a significant fraction of water was lost from bedded salt specimens after irradiation. However, for pure salt the loss of water observed was insignificant. This water loss in bedded salt after irradiation was a result of thermally induced migration of brine cavities and/or expulsion of the brine or steam along crystal boundaries. Experiments on retaining radiation defects within sodium chloride indicated that no chlorine had escaped from the crystals during irradiation or annealing.

In a later study, Jockwer and Mönig (1993) used 1.5×10^6 Gy of gamma radiation to irradiate rock salts with a mineralogical composition of 95 wt % halite and 5 wt % anhydrite,

polyhalite, and kieserite. The overall mean content of water was approximately 0.04% and included the water because of the presence of hydrated minerals, such as polyhalite and kieserite, and adsorbed water at the crystal boundaries or trapped as small inclusions. The presence of HCl and other gases could even be detected at temperatures below 100°C. There was an apparent correlation between the enhanced gas release and the decomposition of the minor minerals that contained water of hydration (i.e., polyhalite and kieserite).

Gies and colleagues (1994) performed *in situ* experiments in which they irradiated rock salts with ^{60}Co sources that had an initial average activity of 3.145×10^{14} Bq (2×8500 Ci per borehole) and heated these salts. These experiments lasted 2 years. The highest cumulative dose was of the order of 10^8 Gy. On a wt % basis, the average mineralogical compositions of the salts surrounding the borehole were as follows:

- halite, 92.8%–96.6%;
- anhydrite, 0.5%–5.5%;
- polyhalite, 1.9%–6.7%;
- total water, 0.12%–0.44%; and
- adsorbed water, 0.01%–0.05%.

For these salts, sodium and chlorine concentrations were also determined and were found to vary between 37.9 wt % and 39.19 wt % for sodium and 57.15 wt % and 60.23 wt % for chlorine. Researchers detected no chlorine by direct *in situ* measurement of the gases released from the rock salts and fluid. They applied special chemical methods, such as iodometric titration and UV-VIS spectroscopy, to measuring the hypochlorite ion, which is formed in the irradiated salts when they are dissolved in water. Neutral chlorine atoms react with water to form one-half equivalent of hypochlorite and one-half equivalent of chloride ions. Composite samples located closest to the ^{60}Co radiation source (No attempt was made to separate colored from uncolored crystals.) averaged 0.4 μmol neutral chlorine atoms per gram of salt, a factor of two more than other positions.

UV-VIS analysis was carried out after mechanically separating colored and uncolored crystals. This analysis revealed greater neutral chlorine (up to 2 μmol/g) of more than a factor of ten in colored halite, as compared to adjacent uncolored crystals. The colored halite indicates the formation sodium colloids. Gies and colleagues (1994) determined that whenever a piece of salt is blue, it contains greater than 10^{-5} mol % of sodium colloids; but the salt is yellow, the sodium colloid concentration is less than that. Higher concentrations of sulfates in salts reduced the degree of radiation damage. Researchers also compared qualitative and quantitative aspects of natural halite decomposition by radiolysis, basing their theoretical predictions on the Jain-Lidiard model (Jain and Lidiard 1977) for moncrystalline crystal. Generally, they found good agreement between the theoretical model and the experimental

results, except in case of polycrystalline salts in which the theoretical model could not explain all the effects.

The interstitial chlorine bubbles and colloidal sodium formed in the salt crystals after prolonged exposure are both chemically very reactive. Brewitz and Mönig (1992) suggested, based on the experiments on high-activity waste (HAW) tested in the Asse mine, that chlorine may diffuse through the crystals and may eventually be released into the borehole. However, colloidal sodium can react with water molecules (if present on the intercrystalline boundaries) to form hydrogen. The yield for the conversion of radiation into chlorine bubbles was not known, but it appeared to be fairly small (below 5%). Because the generation of hydrogen was just one of the possible reactions, the gas yields were lower than expected. Moreover, researchers had to take into account that only parts of the produced gases ended up in the emplacement borehole. If both hydrogen and molecular chlorine were released from the salt into the gas phase, HCl might form (Jenks and Baes 1980). Jenks and Baes observed neither HCl nor chlorine in the flue gas. They found the permeability and the porosity of the gas to be independent of the mineralogical content.

Akram and colleagues (1992) also showed that various parameters influence gas-production rates in rock salt samples. Such factors include integrated dose, dose rate, irradiation temperature, grain size, composition of the rock salts, and fluid inclusions. To simulate the real energy spectrum of HAW, they used spent fuel elements in a reactor for irradiation of rock salts. They quantified the generation of various gaseous components (CO_2, N_2O, CO, hydrogen, hydrocarbons, chlorine, HCl, H_2S, and SO_2). According to Akram and associates, the origins of these gases could be traced back either to radiolysis, thermal desorption, or gas liberation from fluid inclusions in rock salt. They observed chlorine gas production only above 10^7 Gy.

The grain size of crushed rock salt ranged from ($0.125 \text{ mm} < d < 0.25 \text{ mm}$) to ($4 \text{ mm} < d < 8 \text{ mm}$). Small-grain samples produced more gas than large-grain-size samples because in small salt particles the radiation penetration before energy loss is more complete than with large particles. Akram observed that the probability of gas or fluid leakage out of rock salt from fluid inclusions was higher with small-size particles before and during irradiation.

For highly penetrating γ radiation, it is possible that with the small salt particles, more gas is being formed close to the particle surface and may be diffusing out before other reactions occur. These experiments also indicated that the sodium-colloid formation was maximum at 150°C. The dose rate had minor influence on sodium-colloid formation at 150°C, but the total colloid formation was proportional to the integrated dose. Fourier-transform infrared (FTIR) spectroscopy was used as an analytical technique for gas analysis. It offered low detection limits and fast and simultaneous multigas determination, especially for reactive radiolytic gases. However, Akram and associates (1992) did not report actual values for chlorine and HCl gas.

Rothfuchs and colleagues (1995) studied radiolytic generation of gas, such as chlorine and colloidal sodium, by irradiating salt samples taken from a high-level radioactive waste repository in Germany. For their irradiation experiments, they used ^{137}Cs and ^{90}Sr. They irradiated the samples between the temperature range of 100°C to 250°C. At each temperature, they varied the dose between 10^6 and 10^8 Gy. This study confirmed unequivocally that the radiation products colloidal sodium and chlorine were formed in equal amounts (on molar basis) over the range of temperatures and radiation doses investigated. Researchers concluded that, at temperatures above 150°C colloid formation starts to saturate with increasing temperature. At lower temperatures of 100°C, approximately 0.7 mol % sodium was detected for 10^8 Gy but no saturation was indicated. Most of the molecular chlorine after irradiation was in the bulk solid, but the diffusion of chlorine from the salt increased with temperatures. The stored energy increased with the total dose. Researchers derived a conversion factor of approximately 70 J/g per mol % colloidal sodium in the rock salt (Rothfuchs et al. 1995).

As mentioned previously, Pederson and colleagues (1986) found that, assuming no significant loss of neutral chlorine takes place from the host salt after irradiation with ^{60}Co γ rays at an integral dose of 10^9 rads, equal quantities of base (NaOH) and acid (HCl and HOCl) were created upon dissolving the salt in water. After disproportionation of OCl^- to ClO_3^- and further reactions, researchers expect no impact of radiation damage on the pH of brine. One hypochlorite ion is produced for every two neutral chlorine atoms created in the salt by radiation damage.

Kelm and Bohnert (1996) irradiated NaCl salts with ^{60}Co at room temperature for total doses ranging from 0.1 up to 7×10^6 Gy at three different dose rates of 0.1 up to 7×10^3 Gy/h. For NaCl, only tiny amounts of gases were formed after irradiation because the residual water content was so low at only 0.015 wt %.

In dry NaCl, the radiation energy is stored mainly as F and H centers. Upon dissolution, they undergo complex reactions. Kelm and Bohnert found the yield of ClO^- to be less than 10% of the net radiolytic effect. The concentration of ClO^- increased with the dose and was found to be independent of the dose rate, even though the color of the samples was different at higher dose rates. The agglomeration of F and H centers, which is indicated by the shift of light absorption to longer wavelengths, did not seem to influence the yield of ClO^-. Approximately 60 µmol of ClO^- were formed per mega joule (MJ) absorbed radiation energy, equaling a G value of 0.0006. At the lowest dose, the yield of ClO^- was approximately 2.7 times higher.

Kelm and Bonhert suggested that an early stage coloration generally occurs as a result of the relatively rapid accumulation of F centers in salt specimens when they are irradiated. Saturation of this stage occurs at approximately 10^{17} centers/cm^3, corresponding to approximately 0.008 cal/1 g at 5 eV/center. This stage is thought to result from the conversion of other defects, which are already present in F centers. The amount of early stage coloration

in NaCl is also affected by several factors, including temperature, impurities in the salt, and prior plastic strain in the salt (Clark and Crawford 1973).

Vainshtein and colleagues (1997) recently observed the formation of void and void structures in heavily irradiated NaCl under electron irradiation. Natural rock salts and KCl were among the salts irradiated with 1.35 MeV electrons from a Van de Graaff accelerator. Irradiation doses up to 1.5×10^9 Gy were applied at temperatures between 30°C and 150°C. The samples were 6 mm in diameter and were 0.5–1 mm thick. Under these irradiation conditions, up to 15% of NaCl crystal was reported to be transformed into elemental sodium and chlorine.

Researchers observed voids with sizes between 0.05 to 0.7 μm in many irradiated samples. However, in heavily irradiated natural rock salts, very large voids with diameters from 1.2 to 5 μm were created. The size, shape, and distribution of the voids depended strongly upon the irradiation dose, irradiation temperature, and the presence of impurities. The small, randomly distributed voids observed in the earlier stages of irradiation were transformed with increasing doses into a more or less regular void lattice. The lattice of these voids was similar to the one of NaCl along the same axes (7.2 mol % colloidal sodium).

Den Hartog and Vainshtein (1997) found that the size and density of the voids did not saturate for KBF_4-doped NaCl crystals, even when the crystals were irradiated at doses up to 1.5×10^9 Gy. These sodium and chlorine precipitates and void structures are accompanied by the accumulation of stored energy with a maximum of ~78 KJ/mol. Researchers proposed that possibly the collapse of large voids initiates an explosive release of stored energy, giving rise to a localized hot spot and a thermal shock wave. These explosions in NaCl were explained by a number of features of the damage centers in which shock waves in heavily damaged NaCl induce very localized and coherent back-reactions between sodium and chlorine. These reactions amplify the strength of the shock wave. The presence of voids (not the chemical reactions) effectively feeds energy to the shock wave. Therefore, extremely small, nanometer-sized, and radiolytic sodium and chlorine precipitates are important reaction products that give rise to very fast local reactions and transfer of chemical energy to the shock wave, which in turn leads to explosive decomposition.

Paparazzo and colleagues (1997) used Scanning Auger microscopy (SAM) and reflected electron energy-loss microscopy (REELM) to study the chemical changes induced by low-energy 10-keV electron bombardment at the surface of the following alkali halides: LiF, NaF, NaCl, and KI. With SAM, the alkali-to-halogen surface ratio was shown to increase with the irradiation time. This result suggests that as halogen is liberated, the electron bombardment produces an accumulation at the surface of the alkali metal. However, this chemical change could not be monitored by high-resolution spectra.

Several researchers have reported the sputtering of chlorine, sodium, and sodium chloride from the surface of NaCl crystals during exposure to low-energy electrons in a highly

evacuated environment (Elliott and Townsend 1971, Tokutaka et al. 1970). However, investigators who exposed NaCl to high doses of fast electrons or to γ rays while NaCl was sealed within evacuated ampoules, could not detect chlorine in the irradiated ampoules by sensitive mass spectrometry (MS) (Didyk et al. 1971, Compton et al. 1972). No explanation was offered for the apparent differences between the two types of experiments. The adsorption of the chlorine in the later experiment, on either the inlet of the MS or the ampoules itself, could have been responsible for chlorine not being detected.

High-LET Radiation Sources (α particles, protons, deutrons, and others)

Dreschhoff and Zeller (1977) bombarded single crystals of NaCl with 1- to 2-MeV protons with a flux of ~10^{12} protons/cm^2/s and an integrated dose of approximately 10^{15} particles/cm^2 from a Van de Graaff accelerator at low temperatures and at room temperature. They found that, in the case of low temperature, a layered structure developed within the irradiated part of the crystal. They studied the color-center distribution in the irradiated area along the particle trajectories. The following three zones were visible:

- a strong color-center development in the upper region,
- a colorless layer, and
- a deeply colored zone caused mainly by severe lattice damage.

During irradiation, the terminal layer constituted a region of positive charge, which gave rise to a second-order Stark effect. This effect resulted in the annihilation of F centers immediately above this zone and was therefore responsible for the observed decoloration. Investigators observed a similar transparent zone after α-particle irradiation. In the case of proton irradiations, they observed that the F-center concentration continued to increase up to a maximum proton dose of approximately 10^{15} protons/cm^2. Continuing the irradiation beyond this dose resulted in a decrease in F-center concentration, coincident with the formation of a U center.

Study of the damage in single NaCl crystals during continuous irradiation by a 1-MeV ^{4}He ion beam showed that the radiation damage increases up to a dose of 10^{15} to 10^{16} α particles/cm^2 and then reduces thereafter (Hollis 1973, Newton and Hay 1980). The various tests indicated that the radiation damage to NaCl saturates at a dose of approximately 10^{15} α particles/cm^2, a condition which is possibly caused by the recombination of F centers with interstitial halogen atoms (Newton and Hay 1980, Newton et al. 1976).

Researchers have shown that the irradiation of KCl with 2.5-MeV protons at temperatures in the 150°C–220°C range led to the formation of F centers and colloid particles (Bird et al. 1981, Wardle 1975). Researchers observed a rapid growth to saturation of the F-center

population, followed by colloid formation. Both the F-center saturation level and the growth rate of colloids had strong temperature dependence with the peak later observed at 170°C.

Price and Kelly (1978) saw a significant difference in damage after prolonged irradiations of alkali halides with $^4He^+$ and protons. Irradiations with protons using a Van de Graaff accelerator on NaCl (0.7 MeV) and KCl (1 MeV) showed no evidence of recovery of the damage up to doses of 10^{16} ions/cm^2. In contrast, for 1 MeV, α particles showed no plateau with increasing dose, but they did show a recovery of the damage in the previously mentioned salts. For 1-MeV α-particles, the F centers saturate at 10^{14} ions/cm^2. For proton irradiations, the damage is in two stages. The first stage is apparently caused by indirect displacements and saturates at ~10^{15} ions/cm^2. The second stage is attributed mainly to cascades. In the case of α particles as compared to protons, there is a higher rate of damage and an earlier saturation for crystals with atoms of unequal mass (NaCl).

Wardle (1975) found that for aged salts that were initially irradiated with either 2.2 MeV ^{3}He ions at a dose of 5×10^{16} ions/cm^2 or 1.5 MeV protons at a dose of 4×10^{16} ions/cm^2, there was an appearance of a second minimum-maximum pair within the original F- and M-center minima near the end of the range in heavily irradiated samples. Immediately following the irradiation, a colorless layer formed, indicating a minimum in the F- and M-center concentrations. The layer formed at the end of the α-particle or proton range, where the damage to the crystal lattice is maximum and is attributed to the local annihilation of these saturated centers by helium substitutes, such as He^0 or He^- for α particles and formation of U centers for protons. Because large amounts of energy are deposited in this volume of the crystal, the greatest concentration of extended defects (such as dislocations, cracks, and voids) are expected to occur here. Significant annealing of these defects would not occur at temperatures well below the melting point of the crystal; they are expected to persist even when the F centers are annealed (Wardle 1975).

According to Weber and colleagues (1995), the optimum temperature (150°C) for colloid formation in CaF_2 under α-irradiation conditions (~ 5×10^6 Gy/h) was significantly higher than the peak temperature (60°C) reported for colloid production in electron-irradiated CaF_2 at slightly higher dose rates (~10^7 Gy/h). The observed shift to higher temperatures and doses for colloid formation under α irradiation may be caused by helium introduced as the α particles come to rest. If helium is trapped in F centers, then higher doses and temperatures may be required to produce colloids. Additionally, trapped helium may stabilize the anion voids to higher temperatures. The production of Frenkel pairs on the cation sublattice by elastic (ballistic) collisions could also shift the dose-dependent temperature. These results suggest that determining an optimum temperature for colloid formation in alkali metal and alkaline-earth halides under specific conditions of irradiation is extremely critical.

Weber and associates (1995) also observed an initial increase in average colloid radius with temperature for CaF_2 under α irradiation. The colloid radius attains a maximum at a certain temperature and begins to decrease again. Under alpha irradiation for CaF_2, the colloid radius

is also maximized at a temperature of 150°C. The observed change in colloid radius with temperature is consistent with the predictions of the Jain-Lidiard model (1977) for radiation-induced colloid formation in NaCl.

Molten Salt Reactor Experiment

Another concern was the long-term storage of frozen fuel salts from the Molten Salt Reactor Experiment (MSRE) at Oak Ridge National Laboratory. The storage of these large quantities of fluoride salts that were contaminated with substantial-level radioactivity could generate enough gas pressure through radiolysis to compromise the integrity of the containment system (Notz 1988, National Research Council 1997, Toth and Felker 1990, Williams et al. 1996). After being used as MSRE fuel, these salts, with their original composition of LiF(64.5 mol %)-BeF_2(30.3 mol %)-ZrF_4(5 mol %)-UF_4 (0.13 mol %), have large enough amounts of other actinides and fission products to cause radiolysis of the salt and accompanying release of fluorine gas. Preparing these salt mixtures involved heating the salts at approximately 100°C above liquid point of the mixture to form a homogeneous solution and then cooling the mixture.

First, this process is similar to the calcination of PuO_2 at 950°C, which is approximately 100°C above the melting points of various possible alkali and alkali-earth chlorides (e.g., NaCl, KCl, LiCl, $CaCl_2$, $MgCl_2$, and others). Although, PuO_2 remains insoluble and external to the alkali halides while in the MRSE salts, the α-emitting ^{233}U is complexed with the crystal lattice. Secondly, the salt mixtures consist of alkali and alkaline-earth halides. These are two of the main reasons the studies related to the MSRE project are of interest to the present project. However, the quantities of materials (salts and radionuclides) and the total thermal output caused by various radiation sources in actual MSRE containers are several orders of magnitude higher. Furthermore, fluorine gas generation and recombination rates were controlled by the concentration of defects within the salt lattice itself, instead of by the conditions external to the crystal lattice, as is the case of storage of PuO_2 and alkali-halide mixtures (Toth and Felker 1990).

The models for generating gas for MSRE are based on laboratory experiments for powdered fluoride salts that have been exposed to large doses of γ radiation; these experiments suggest 2 mol % as the maximum limit of damage to crystalline material (Notz 1988, Toth and Felker 1990, Williams et al. 1996). This determination was based on the amount of fluorine gas released (Notz 1988, Toth and Felker 1990). At this point, the rate of fluorine gas recombination with the active metal centers was equal to the fluorine generation. At 150°C, the recombination rate of fluorine gas should equal the rate of generation under those conditions. For lower dose rates, this temperature would be lower.

Based on several experiments involving radiolysis of MSRE salts with various radiation sources at room temperature, Williams and colleagues (1996) suggested a consensus value of fluorine gas yield (i.e., G [F_2] = 0.02 molecules/100 eV of deposited energy). Initial results of

plutonium, α-irradiated MSRE did not indicate any fluorine gas generation; but researchers advise treating all the radiation sources as being equally effective in causing radiolysis. Activated charcoal may give favorable results as a possible getter for fluorine (Notz 1988). The G (F_2) = 1.5 molecules/100 eV were reported for α irradiation in solid UF_6 from actual MRSE experiments (National Research Council 1997, Trowbridge et al. 1995). Large quantities of F_2/UF_6 have so far been collected in actual MRSE salts (National Research Council, 1997).

Other Matrices

Lewis and associates (1993) showed that chloride-salt-occluded zeolites used as immobilization media for the salt waste from spent fuel for the integral fast reactor (IFR) to be radiation stable at γ doses of 10^7 Gy. These zeolites prevented the coalescence of color centers formed in alkali chloride after irradiation from yielding metal colloids and interstitial chlorine. The zeolites also enhanced the radiation stability of occluded salt.

Lewis and Warren (1989) investigated, for radiation effects, a mortar formulation capable of immobilizing chloride salts with a high level of radioactivity. They determined the radiolytic generation of gas(es) from the irradiated mortar for several formulations with variable salt loadings at several test temperatures. The irradiation of mortar, consisting of cement, slag, fly ash, water, and 0 wt %–10 wt % salt led to the generation of hydrogen. The salt mixture was 56 wt % KCl- and 44 wt % LiCl. They irradiated the mortar with ^{60}Co γ rays at dose rates varying from 0.1 to 0.5×10^4 Gy/h for up to 4500 h. The rate of hydrogen generation increased with increased salt loading of the mortar. These results were consistent with the mechanism in which the hydroxyl radicals (which are supposed to neutralize hydrogen molecules) react with scavenger species, such as chloride ion, in the mortar. Experiments on aqueous and concentrated brines suggest the following hydroxyl-chloride reactions (Lewis et al. 1993, Lewis and Warren 1989):

$$OH\cdot + Cl^- \rightarrow ClOH^- \quad , \qquad (26)$$

$$H^+ + ClOH^- \rightarrow Cl\cdot + H_2O \quad , \qquad (27)$$

$$Cl\cdot + Cl^- \rightarrow Cl_2^- \quad , \text{ and} \qquad (28)$$

$$2Cl_2^- \rightarrow Cl_2 + 2Cl^- \quad . \qquad (29)$$

Lewis and Warren concluded that, if the hydroxyl radical-chloride ion reaction occurred in the mortar matrix, an increase in hydrogen yield would follow an increase in the chloride concentration. This increase would occur because the recombination reaction of the hydrogen and hydroxyl radicals would be inhibited. Experimental results at room temperature supported this theory. However, the researchers detected neither oxygen nor chlorine gas in

the gas phase, indicating that the mortar matrix influences the overall reaction mechanism and the final irradiation products.

Lewis and Warren also found that the rate of hydrogen generation decreases with temperature and chloride-salt concentration. A possible explanation for these results was that greater amounts of chlorine may be formed from the chloride salts in the mortar at the higher temperatures.

Scavenging reactions among the chlorine and the hydrogen precursors, the solvated electron, and the hydrogen radical may be enhanced, thereby reducing the yield of hydrogen (Lewis et al. 1993, Lewis and Warren 1989). This mechanism can be represented by

$$e_{sol}^- + Cl_2 \rightarrow Cl_2^- \quad , \qquad (30)$$

$$e_{sol}^- + Cl_2^- \rightarrow 2Cl^- \quad , \text{ and} \qquad (31)$$

$$H\cdot + Cl_2 \rightarrow H^+ + Cl^- + Cl\cdot \quad . \qquad (32)$$

This low hydrogen yield was also supported by the fact that approximately 50% more chlorine was formed interstitially in the solid salt at 150°C than at room temperature.

Radiation-Induced Thermal Effects in Salts

In general, a majority of the energy of radiation absorbed for each chemical bond that is broken appears as ~80% heat and only a small fraction of this energy is actually required to break the bonds.

Molecke and Sorensen (1989) studied the thermally induced breakdown of magnesium-chloride impurities and hydrated forms thereof in host rock salt from the Waste Isolation Pilot Plant (WIPP). They showed that these salts release measurable quantities of HCl (10 ppm).

Pederson (1986) and associates found that the influence of heat from the waste package is potentially more important than radiation damage. Heating natural rock samples with high concentrations of Na^+, K^+, Ca^{2+}, Cl^-, and SO_2^{2-} causes acidic gases (such as HCl, SO_2, and H_2S) to evolve, leaving behind a highly basic salt.

In laboratory experiments with crushed salt used for backfilling, Gommlich and colleagues (1995) found that HCl was released when heated beyond 80°C. However, they found no HCl in the field test (less than detection limit of 1 cm^3/m^3), possibly because all the HCl may have reacted with the steel casks, a condition that led to the generation of hydrogen.

Plutonium Dioxide

The plutonium dioxide in plutonium storage containers exists as fine particles in the micron range. Heating in air at 950°C to remove water, hydrocarbon, and other volatile species processes plutonium oxide. The particle size of PuO_2 is a function of its history and some materials may have much smaller sizes than others. Surficial water is re-adsorbed when the oxide is exposed to room air during packaging operations (Haschke 1996, Haschke and Ricketts 1995). The surface area of fired oxides is low, less than 5 m^2/g. Therefore, the water adsorption is limited to 0.2 mass % at 50% relative humidity (Haschke and Ricketts 1995). Haschke and Ricketts suggested that radiolysis of this water to oxidation/reduction products leads to the higher oxidation states of plutonium. As a result, a mixture of Pu(IV) and Pu(VI) is obtained. This phenomenon is only possible on the surface of plutonium, although the stoichiometry of PuO_2 can vary over a small range.

Phase II

Significance of the Radiolysis Literature Review to Long-Term Storage of PuO_2 Accompanied by Halide Salts

Abstract

The Material Identification and Surveillance (MIS) project sponsored a literature search on the effects of radiation on salts, with focus on alkali chlorides. The goal of the survey was to provide a basis for estimating the magnitude of alpha (α)-radiation effects on alkali chlorides that can accompany plutonium oxide (PuO_2) into storage. Phase II of this report deals with the core issues pertaining to radiolysis of chloride salts in the storage environments.

According to DOE-STD-3013 technical standard, "Criteria for Preparing and Packaging Plutonium Metals and Oxides for Long-Term Storage" (1996), chloride radiolysis can yield potentially corrosive gases in containers that can adversely affect the long-term stability of containers. The standard states that a maximum of 5.0 kg of plutonium-containing material previously calcined at 950°C or higher for at least 2 h is to be stored in welded stainless-steel (300 series) containers. The maximum permitted thermal output is 30 watts (W) in the inner container that is sealed and then placed within a welded container to be stored for a maximum of 50 yrs at a steady-state (elevated) temperature of PuO_2.

For purposes of this project, the key factors are the maximum permissible moisture content of PuO_2 at 0.5 %, the maximum observed thermal output of 10 W, and the salt content of NaCl, KCl, $MgCl_2$, $CaCl_2$, etc. The salt content is reported in actual material to be as high as ~20% initially, but is considerably reduced on calcining.

The goal of this project is to predict the extent of adverse effects of radiolysis of salts accompanying the PuO_2, including the consequences of energy stored in these salts and the quantity of chlorine gas, hydrochloric acid (HCl), or other corrosive oxychlorides formed during the storage lifetime (50 yrs). If significant quantities of these species are present, corrosion or stress-cracking in the inner container can result.

To predict the amounts of the corrosive chloride species formed in the DOE-STD-3013 containers as a result of radiation damage to the salts, one needs to know either the experimental or the theoretical G values. However, studies on the effects of α radiation are relatively few when compared to the extensive literature on effects of more penetrating beta (β) particles, x-rays, or gamma (γ)-ray radiation. It is important to consider the various transient species and the reaction scenarios. Information based on several years of practical experience with these materials at Los Alamos National Laboratory (LANL) and other DOE sites is discussed. Results from headspace gas analysis of actual containers received from Hanford Site are also discussed.

Introduction

Long-term radiolysis effects need to be addressed because we propose to store mixtures of PuO_2 and chloride salts for a period of 50 yrs. We undertook an extensive survey of pertinent radiolysis literature. Of significance to storage is high specific activity alpha (α) mixed with chloride impurities. Literature reports in which the interaction of α particles with high-salt environments have been studied are limited. Therefore, the conclusions in this report are largely based on the radiolysis effects with salts and rock salts (>95% halite) using the more penetrating radiation: gamma (γ) rays, x-rays, electron interactions, or proton irradiations.

In general, α-radiolysis effects in solids are confined to a shorter range and generate higher G values than γ or electron radiolysis. As the weapons-grade material with typical isotopic composition of ^{238}Pu (0.008 wt %), ^{239}Pu (94.2 wt %), ^{240}Pu (5.7 wt %), ^{241}Pu (0.11 wt %), ^{242}Pu (0.02 wt %), and ^{241}Am (0.17 wt %), "ages" in the next 50 yrs, radiation dose caused by low linear-energy-transfer (LET) beta (β) particles and γ rays might have to be taken into account. However, the β activity falls by half in 14 years. In PuO_2 with isotopic composition similar to the one already mentioned the α and the low-energy β-specific activities are comparable. Together with α, β, γ, and electron irradiation of the salts, one also might take into account the gas phase irradiation of the air above the material. Moreover, the energy deposited by the low-energy β particles and γ rays would be very small when compared to α particles.

Very little in the literature reports deals with the radiation effects of salts in fine grains. With small-particle salt samples, as in the case of plutonium storage, single crystalline effects might not be valid. Also, we found a limited number of references for brine interactions with actinides, radiolysis in salt-occluded zeolites, and salt cakes. A few reports from the Molten Salt Reactor Experiment (MSRE) were helpful. For salts, significant radiation damage can easily be observed because irradiation induces color centers that can coalesce to form metal clusters, colloids, and chlorine.

The key issues of relevance to the present literature search are

- the formation of F centers,
- coloration,
- sodium colloid formation,
- energy deposits in the salt, and
- generation and escape of chlorine gas from the crystal lattice.

The gaseous chlorine is highly reactive with moisture, even in trace amounts. This reaction leads to the formation of HCl and other corrosive oxyanions. The presence of impurities in the material, the particle sizes of PuO_2 and of the halide salts, and especially the temperature

are the most critical factors that have to be considered to predict the yields of corrosive gases. The temperature of the materials inside the containers will depend on the storage conditions. Generally, in isolated containers the temperatures will not exceed 100°C; but, in the midst of an extended matrix of storage containers, the temperatures will approach 150°C or higher (up to 300°C are possible in certain cases).

The dose rate and total absorbed dose are other key issues. The corrosion rates are probably influenced by the generation of transient species that will affect pH and/or Eh of the available moisture and air.

Predicting Radiation-Induced Gas Generation in Plutonium Storage Containers

1. Extent and Limitation of the Review

The purpose of this review is to present an overview of data on radiation effects, the theory of radiation damage, and the relationships of radiation effects and irradiation damage to the key issues involved in storage of PuO_2 with other constituents, chiefly chlorides. We found that we could use the following guidelines in using the reported research.

- To predict the products of halide radiolysis in plutonium-bearing storage containers, researchers use information obtained from studies on rock salts, pure alkali and alkaline-earth halides, water, and brines.
- In the absence of theoretical or experimental G values for the α-induced radiolysis of salts, the best recourse may be to extrapolate the results using a model based on the data obtained from other radiation damage studies on pure and impure alkali halides and geological rock salts.
- Lacking sufficient experimental data on external α-radiation damage in the salts, to predict α-radiolysis effects with introduction of very little error, researchers can use the more extensive information about the radiation effects on salts caused by γ and high-energy electron irradiations (Kazanjian and Brown 1969, Notz 1988, Sullivan 1983, Turner 1986, Williams et al. 1996).
- Generally, to quantitatively estimate the radiation damage in salts, we had to place emphasis on the literature reports in which the measurements are made during the irradiation. Under certain conditions, it has been shown that once the irradiation source is removed, annealing or recovery of the salts begins immediately (Levy 1991, Levy et al. 1981).
- This paper applies the classical Jain-Lidiard model for radiation damage in salts (Jain and Lidiard 1977). For comparative purposes, radiolytic fluorine gas generation in the

MSRE was also considered (Notz 1988, National Research Council 1997, Toth and Felker 1990, Williams et al. 1996).

- We also took into account results of headspace gas analysis from Hanford Site materials, as well as observations based on several years of experience handling these materials at LANL.

2. Observations Using the Actinides as Radiation Sources

In plutonium intended for storage with isotopic composition similar to ^{238}Pu (0.008 wt %), ^{239}Pu (94.2 wt %), ^{240}Pu (5.7 wt %), ^{241}Pu (0.11 wt %), ^{242}Pu (0.02 wt %), and ^{241}Am (0.17 wt %), the β activity is often comparable to that of the α activity. This β activity, caused by ^{241}Pu, falls by one half in 14 years. Also, β particles are relatively weak in energy (a few hundred eV) and, consequently, do not deposit comparable amounts of energy. Natarajan and colleagues (1989) conducted studies about thermally stimulated luminescence (TSL) on ^{239}Pu- and ^{241}Am-doped NaCl and KCl and compared the results with γ-irradiated salts. In general, researchers found for these salts that the TSL glow pattern of the ^{239}Pu- and ^{241}Am-doped salts and γ dose-dependent peaks and trap depths were similar.

In contrast, when divalent metal fluorides (such as BaF_2,, CaF_2, CdF_2, and SrF_2) are subjected to α, electron, or x-ray irradiation, F centers and metal colloids are the principal types of localized defects first formed (Exarhos 1982). The cross-section for creating a particular defect depends upon the type of ionizing radiation. Colloid formation is favored under electron excitation, whereas it might be suppressed under α excitation or when the crystals undergo additive coloration (Exarhos 1982, Thompson et al. 1978).

One of the rare studies involved radiation damage to electrorefinined residues that contain Pu(III) in KCl, where plutonium is actually incorporated within the salt matrix involved (Morris et al. 1989). The plutonium had similar isotopic composition as the PuO_2 intended for storage in plutonium storage containers. Researchers compared radiation-induced color changes with those in lanthanide-doped (lanthanum, neodymium, gadolinium, and lutetium) and undoped KCl when these PuO_2 salts were subjected to intense γ radiation. Even though they observed similar color changes for both α-irradiated and γ-irradiated samples, the nature and intensity of F-center production were different. They believed the basic differences in mechanisms for radiation damage observed with various radiation sources to be responsible. As will become evident, the literature on radiation effects does not always present a consistent picture of cause and effect. These results reaffirm that one needs to exercise caution in predicting the α-radiation yields of species in impure PuO_2, based on data and models in which the primary source of radiation was other than α radiation.

3. Relationship of High-LET Alpha Radiation and Low-LET Radiation Sources

Price and Kelly (1978) found that alkali halides bombarded with high-energy protons, deuterons, or α particles from an external source can be used to predict radiation defects. However, one has to keep in mind that the defects will be formed by both direct and indirect displacement mechanisms.

Roberts and associates (1981) showed that using ion bombardment will lead to a homogeneous distribution of radiation damage. Because of the limited range of these ions in solids, one can end up studying only the radiation damage on the crystal's surface.

Wardle (1975) found that additional phenomena (such as sputtering, channeling, and the formation of U centers for proton irradiation) also may have to be taken into account when using ion bombardment. The later phenomena are not important in cases of electron, γ-ray, or x-ray irradiation or with the α-doped salts.

Williams and colleagues (1996) suggested (based on heat-transfer studies) that, if larger chunks of salts are used instead of smaller-sized grains, considerable heating occurs that promotes the recombination of the halogen gas.

Saturation effects can limit the amount of damage to the alkali-halide crystals but can vary with the nature of incident radiation (Levy and Kierstead 1984, Luntz et al. 1977, Thompson et al. 1978, Wardle 1975). Saturation produces a practical limit to the number of vacancy-type centers that can be introduced into the lattice. Levy and Kierstead (1984) observed higher radiation damage rates in rock-salt surfaces by a factor of 10 to 10^3 for α-particle irradiation, as compared to γ-ray exposure. This higher damage rate will likely lead to saturation of radiation defects for α-irradiated salts at lower doses and irradiation times.

Depending on the energy of the α particles and protons for various ion-bombardment experiments in NaCl and KCl, the saturation fluence is reported to be 10^{16} ions/cm^2 (Bird et al. 1981, Dreschhoff and Zeller 1977, Hollis 1973, Newton and Hay 1980, Newton et al. 1976, Price and Kelly 1978, Wardle 1975). Saturation concentrations for KCl irradiated with 1.5-MeV protons and 1.5-MeV α particles were comparable: 1.3×10^{19}/cm^3 and 1.4×10^{19}/cm^3, respectively. These minor differences were attributed to the high-instantaneous electron-hole concentration in an ion infratrack (Luntz et al. 1977, Thompson et al. 1978), even though the alpha particles have four times the LET of the protons of the same energy (Turner 1986).

With higher energies, for the same fluence the number of F centers produced by 2.3-MeV protons are approximately twice as many as those produced by 2.3-MeV α particles (Luntz et al. 1977, Thompson et al. 1978). Also, LET decreases with increasing α-particle energy above 1.5 MeV. The F-center saturation in positive ion bombardment is an order of magnitude higher than that reached in x-rays or in MeV electrons. This is again attributed to

high-electron-hole concentration in an ion infratrack (Thompson et al. 1978). F-center production efficiency in KCl at room temperature for electron-beam irradiation is 1.75 times greater than that for γ-ray irradiation under similar crystal conditions (Luntz et al. 1977).

4. Predictions of Alpha Damage in Chloride Salts Stored with PuO_2

To make a meaningful comparison with the literature reports on radiation damage to the salts, it is critical that the dose (perhaps dose rate) in plutonium storage containers be comparable. Also, care must be taken to ensure that the relevant crystal parameters, crystal conditions, and temperature are comparable (Luntz et al. 1977). A damage model based on certain simple assumptions can be used to predict the generation of corrosive gases (such as chlorine or HCl) in a plutonium storage container. The assumptions include the following:

- The actinides, salts, water, and other impurities are uniformly distributed in the container.
- All the energy of the α particles will be absorbed by the stored material itself because of the short ranges of the α particles. This energy absorption is clearly a maximum effect and is diminished by energy loss in the PuO_2 itself, as well as being increasingly limited by the penetration into the halide salt crystals as their size exceeds the α range. Loss of energy to the container walls, to the air above the material, and to the surroundings is presumed to be negligible.
- Allow for the 50-year growth of ^{241}Am, which increases but does not double the α-energy from plutonium.

For pure plutonium oxide, the principal sources of radiation in the inner plutonium storage containers will be ^{238}Pu, ^{239}Pu, ^{240}Pu, ^{241}Pu, ^{242}Pu, and ^{241}Am. The α decay in these containers produces energetic α particles (4.5–5.5 MeV), energetic recoil nuclei (70–100 keV), and some γ rays. The average (~5.2 keV) and maximum energy (~20.8 keV of the β particles emitted by ^{241}Pu (14.4 yr, half-life) is very low. For the purposes of dose calculations and of their overall contribution, radiation damage can be ignored. To calculate the integrated dose over a period of 50 yrs in such a container, we used the plutonium isotopic results on a weight-percent basis (from an actual Hanford sample [ARF-102-85-295]). These isotopic compositions are presented in Table 1.

Table 1. Typical Isotopic Composition for Pure Weapons-Grade PuO_2 from an Actual Hanford Container

Isotope	^{238}Pu	^{239}Pu	^{240}Pu	^{241}Pu	^{242}Pu	^{241}Am
Weight %	0.0076	94.1808	5.6858	0.1069	0.0189	0.166

Leasure and associates (1998) reported plutonium contents between 13% and 87.7% for an array of actual material from the Rocky Flats Environmental Technology Site (RFETS) and the Hanford Site. In the case of ^{238}Pu, which has a half-life of 87.75 yrs, approximately 3.8×10^{10} α particles are emitted per minute per milligram. Plutonium-239 has a half-life of 24,100 yrs and emits approximately 1.4×10^{8} α particles per minute per milligram. The specific activities (in watts/gram [W/g]) of the mentioned isotopes in the material container are shown in Table 2.

Table 2.* Specific Activities (in W/g) for Each Isotope of Plutonium and Daughter ^{241}Am

Specific Activity	^{238}Pu	^{239}Pu	^{240}Pu	^{241}Pu	^{242}Pu	^{241}Am
W/g	0.568	1.93×10^{-3}	7.08×10^{-3}	3.41×10^{-3}	1.16×10^{-4}	0.114

* Adapted from ANSI N15.22-1987, "Nuclear Materials—Plutonium-Bearing Solids—Calibration Techniques for Calorimetric Assay"

For weapons-grade plutonium material, if we assume a 50-yr storage lifetime, the fraction of each plutonium isotope (and americium daughter) that has decayed to daughter nucleus in this time period will be as follows (Table 3):

Table 3. The Fraction of Plutonium Isotope (and Americium Daughter) Decay in 50 Years

Elapsed Time (Years)	^{238}Pu	^{239}Pu	^{240}Pu	^{241}Pu*	^{242}Pu	^{241}Am**
50	0.326	0.001	0.005	0.070	0.00	0.077

* The value is the fraction of the initial ^{241}Pu isotope that has β-decayed to ^{241}Am and then α-decayed to ^{237}Np.

**The value is the fraction of the in-grown ^{241}Am that has subsequently decayed to daughter ^{237}Np.

Assuming the maximum-case scenario from the DOE standard, "Criteria for Preparing and Packaging Plutonium Metals and Oxides for Long-Term Storage," the maximum permitted PuO_2 loading is 5 kg, which is equivalent to 4.4 kg of plutonium metal. Assume this amount of PuO_2 is present in the material container.

Theoretical calculations, using Tables 1–3, provide a "lower end" scenario in which 5 kg of pure plutonium oxide is present in the plutonium storage container. This scenario corresponds to a thermal output of 11 W or kg Gy s^{-1} or an initial dose rate of 2.2 Gy s^{-1} (7920 Gy h^{-1}). Assuming all the energy of the emitted radiation is absorbed by the material itself, the expected cumulative dose for a 50-yr lifetime of the material would be of the order 10^9 Gy. Lower wattages/doses would be observed as halide salts replace the PuO_2 content. This value seems reasonable when compared to calculations performed in 1996 for a series of actual materials for which thermal output varied between 0.32 W to 10 W. The "high end" maximum is 30 W/5 kg. According to the DOE standard, "Criteria for Preparing and Packaging Plutonium Metals and Oxides for Long-Term Storage," if the maximum permitted PuO_2 loading of 5 kg for 30 W is assumed, the dose rates and the total dose (without taking decay into account) will still be approximately three times the values obtained here.

The maximum allowable water is 0.5 wt % present on pure PuO_2 in plutonium storage containers. In actual pure PuO_2 material, the water content after calcination is lower and of the same order of magnitude as observed in geological samples for adsorbed water: ~0.04 wt % or even less (Leasure et al. 1998). However, for impure oxides that contain halide salts plus $MgCl_2$, the water content even after calcination might be higher. Indeed, using loss on ignition (LOI) to estimate the water content in impure oxides might not be prudent (Leasure et al. 1998).

According to Haschke and Ricketts (1995), calcination of the oxide at 950°C is effective in removing water and other adsorbates. Moreover, calcination leads to the reduction of the specific area of the PuO_2 particles to a level that prevents excessive re-adsorption of water. Calcination also decreases the source term for environmental dispersal. Irrespective of the nature of water present in the material, if it is adsorbed or absorbed, the radiolysis experiments indicate that the sorbing medium can be either inert to radiation or can transfer all the energy to the sorbed water.

Unless experimental data demonstrate that the binding medium is radiolytically inert (e.g., vermiculite), all the radiation energy should be assumed to interact with the sorbed water (Bibler and Orebaugh 1977). For α radiolysis of liquid-phase water G (hydrogen) range of 1.1–1.6 molecules/100 eV (Bibler 1974, Bibler 1975, Burns and Simms 1981, Spinks and Wood 1990, TRUPACT II SARP 1994). The effect of scavenger impurities, such as NO_3^-, Cl^-, Br^-, and SO_4^{2-}, decrease the yield of G (hydrogen) even more for low-LET γ irradiation than for α irradiation (Bibler 1974, Büppelmann et al. 1988, Gray and Simonson 1984).

The main products from α radiolysis of water in plutonium storage containers are molecular species hydrogen and H_2O_2, with the latter possibly decomposing to yield H_2O and oxygen (Allen et al. 1952, Van Konynenburg et al. 1996). The equilibrium concentrations of the primary products are also going to be very small because a host of secondary reactions will have a net effect of regenerating water (Allen et al. 1952, Büppelmann et al. 1988, Gray and Simonson 1984, Van Konynenburg et al. 1996).

Radiolysis of water adsorbed on the alkali-halide crystals depends on the following:

- the nature of the salt,
- the concentration of the adsorbate, and
- the size of the crystals (Aleksandrov et al. 1987).

Irradiation of alkali-halide crystals that contain adsorbed water will also result in the dissociation of water, thus leading to the formation of the oxide halide on the crystal's surface (Aleksandrov et al. 1987). Salts subjected to doses of 10^7 to 10^8 Gy react with water to form hydrogen gas and other products (Levy et al. 1981).

The adsorbed water on PuO_2 surface is one of the main concerns for this DOE-wide project. A recent review of the literature deals with some aspects of water radiolysis in the plutonium storage containers (Hyder et al. 1998). As stated earlier, studies are currently underway at LANL to address the key issues of water radiolysis in these containers.

A second concern is the radiation effect on the chloride salts that accompany the PuO_2 into storage. Chloride salts arise from pyrochemical purification processes in which molten alkali salts are used. The maximum chloride content reported (so far) for the precalcined samples was ~20 wt %. Calcination of PuO_2 at 950°C (depending on the chemistry of preparation of the oxide) reduced the chloride content by 40% or more. The amount of alkali chlorides distilled away is a function of time, temperature, and equipment design. However, if the draft standard is promulgated as it is currently written, 800°C will be used and the chloride salts will not be driven off. Generally, the chloride content in actual calcined material is <10 wt % compared to rock salts and NaCl that contain ~60 wt % chlorine.

For the purposes of this discussion, it is also assumed that the salts that exist on or around the plutonium oxide are individual salts. The stopping power of water, salts, and other impurities will be higher than PuO_2, and therefore the radiation energy deposited per unit mass (the radiation dose rate) will be proportionately higher. Thus, in plutonium storage containers, it is sufficient to know that the dose rate to the second material will be of the order of the average dose rate in the material (or perhaps higher). A detailed discussion on this matter can be found in Appendix A, "Radiation Dose Rates in Plutonium Oxide."

5. Predicted Radiation Damage and Mechanisms for Gas Generation from the Salts

An estimate of the yield of gaseous products in plutonium storage containers

Expected high-total-dose levels of $\approx 10^9$ Gy would induce the formation of color centers. These color centers depend on the kind of salt impurities present and may vary from blue to blue-black to purple or grayish white. The distribution of these color centers will not be uniform.

These dose levels are above the predicted limit for saturation of radiation damage in salts (i.e., 0.5×10^9 Gy [Soppe et al. 1994]). At these predicted dose levels, the amount of defects formed in the salts in plutonium storage containers may vary from 0.1% to 1 mol % or more (Bergsma et al. 1985, Brewitz and Mönig 1992, Hughes and Jain 1979, Jenks and Bopp 1977, Kelm and Bohnert 1996, Rothfuchs et al. 1995, Spinks and Wood 1990, Seinen 1994).

Under certain conditions, knowing the defect levels present during irradiation is advantageous, rather than theorizing them from data obtained after irradiation (Levy 1991, Levy et al., 1981, Lidiard 1998). This concept was recognized and taken into account to predict radiation damage in plutonium storage containers. However, these observations for radiation damage may be conservative because they are based mostly on lower-energy electron or γ or x-ray irradiations.

Under certain conditions at lower doses by a factor of two or more, Levy and coworkers have reported higher radiation damage for γ- or electron-irradiated rock salts (Levy and Kierstead 1984, Levy 1983, Levy et al. 1983, Levy et al. 1981). However, Levy (1991), in his excellent review article, mentions that if the effective temperature of the salt is either appreciably below or above 150ºC, the amount of radiation damage that he had calculated previously would be lower. This temperature-radiation damage relationship is probably one of the main reasons that our experimental data do not suggest high radiation damage.

In view of limited experimental data, it is possibly safe to assume that for these α-irradiated salts the amount of radiation damage will be higher by a factor of but not exceed 1%–10%. These predictions deal with the worst-case scenario for radiation damage in salts. Therefore, in actual containers at LANL, the extent of radiation damage observed in salts so far is several orders of magnitude less. (See subsequent discussion.)

These values indicate the amount of radiation damage that might possibly form in the salt particle; however, a vast majority of these chlorine centers will be confined to the salt crystal itself. According to reports in the literature, the escape of chloride species (including chlorine gas) from the salt particle is a very inefficient process and depends on the physical properties of the salt itself. These yields are consistent with the model for fluorine-gas generation in MSRE, where researchers have experimentally determined a radiation damage limit of 2% in fluoride salts (Notz 1988, Toth and Felker 1990, Williams et al. 1996).

There are similarities between the MSRE project and the radiolytic generation of fluorine gas, including the salts being mostly alkali and alkaline-earth fluorides. The major differences are that the MRSE actinides are within the salts as complex anions, while the PuO_2 and the salts are separate phases in the material proposed for storage. Under the conditions in a plutonium storage container, a portion of a chlorine gas formed might be released from the salt until a few mol-% damage limits in the crystal are reached.

A simplified picture, based on studies on the MSRE project (discussed in Phase I of this report), is applicable as follows: the formation of radical species by homolytic cleavage of the salt followed by the formation and liberation of homolytic chlorine and the deposition of a resident active metal center in the salt lattice (Notz 1988, Toth and Felker 1990, Williams et al. 1996):

$$\begin{array}{ll} \text{NaCl (or KCl)} & \text{Na}\cdot\text{(or K}\cdot\text{)} + \text{Cl}\cdot \\ \quad + \text{ionizing radiation} \rightarrow & \quad \rightarrow \text{Cl}_2\uparrow \\ \text{MgCl}_2\ (\text{CaCl}_2) & \text{Mg: (or Ca:)} + \text{Cl}\cdot \end{array} \qquad (33)$$

The net production of chlorine gas at the temperatures expected inside the material containers will be limited by the temperature-dependent back-reaction (i.e., recombination) of the metal and chlorine that would restore the original salt. The recombination reactions are expected to take place irrespective of the chlorine gas accumulating within the lattice or escaping to the confinements of a containment vessel (Toth and Felker 1990).

The calcination of PuO_2 salt mixture at 950°C for 2 h lowers the salt content significantly. Also, since the temperature for calcination is above the melting points of most of the possible salts, they might recrystallize as larger particles. This recrystallization will have a significant impact on the extent of radiation damage (Particle size effects are discussed in a separate section later in this report.).

Hydrochloric acid was detected in two of the nine inner containers received from Hanford Site. Using a UTI residual gas analyzer, LANL researchers analyzed the headspace gases before calcination on “as received” material. The levels of HCl in headspace gas are estimated to be very low, several hundred parts per million or lower. (In the absence of an HCl gas standard, only a qualitative estimate could be made.)

One of these containers had the highest salt content (chloride levels), ~20%, in containers analyzed from Hanford so far. These materials have since been thermally stabilized, reanalyzed for physical and chemical content, and placed in storage. The calcination at 950° reduced the chloride levels in the salts from 20% to 7.7%.

These materials were packaged at Hanford in 1985 and were shipped to Los Alamos shortly thereafter. Neither the outer cans nor the inner cans showed any visible signs of stress corrosion or cracking after being stored over a 13-yr period. LANL has been handling the plutonium storage containers from various DOE sites for the past several years. A link between high salt content in the material and visible signs of corrosion has so far not been observed at LANL. Details of the headspace gas analysis of containers from Hanford Site will be discussed in other LANL reports.

Low- to high-dose radiation of alkali and alkaline-earth halides produces H and F centers (halogen interstitial/vacancy pairs) on the halogen sublattice by means of nonradioative decay

of electronic excitations. With prolonged irradiation, this production of H and F centers leads to the formation of chlorine platelets and the precipitation of sodium colloids (Medlin and Howitt 1994).

A simple material balance requires one atom of chlorine to be formed for each atom of sodium incorporated into the colloidal sodium metal particle. The H centers are, in fact, X_2^- complexes (Soppe et al. 1994). Researchers have suggested that the radiation damage in alkali halides includes the formation of interstitial halogen atoms (H centers), which can cluster to dislocation loops and grow into perfect interstitial loops (Egerton et al. 1987, Hobbs 1976, Hobbs 1975, Jain and Lidiard 1976, Newton et al. 1976).

Catlow and colleagues (1980) suggested a two-step model based on defect energies.

1. The first step is the initial aggregation of H centers, in which they form a weakly bound di-H center that collapses into a neutral halogen molecule (X_2) that occupies the interstitial site.
2. The second step involves the creation of interstitial loops by displacing lattice ions to dislocation loops by halogen molecules, which occupy the vacancy created (Hobbs et al. 1972, Seinen 1994).

There is no consensus on the structure of initial aggregates (i.e., if it consists of X_2 or X_3^- molecules) (Catlow et al. 1980). Hobbs (1975) suggested that the number of X_3^- molecular ions is one-half the number of F centers. Aguilar and associates (1982, 1983) suggested a heterogeneous interstitial nucleation model to account for the growth of F and M centers in alkali halides. The migration energy for H centers is 0.1 eV compared to 0.8-0.9 eV for F centers (Levy 1991, Seinen 1994). These different activation energies lead to mobilities that differ by a factor of 10^{10} at 100°C. Therefore, aggregation kinetics is strongly determined by the largely different mobilities of the primary defects.

Levy (1991) found the activation energy for F-center diffusion to be different for natural and synthetic NaCl. For an in-depth analysis of nucleation and growth of F centers and colloids in alkali halides, we recommend a recently published review article by Lidiard (1998), a detailed discussion of which is beyond the scope of this review. A summary of the principal defect reactions contained in his model follows:

I. Salt Irradiation $\rightarrow$ F + H centers ,

II. F + H $\rightarrow$ Complete annihilation ,

III. H aggregation $\rightarrow$ dislocation loops + halogen molecular centers ,

IV. F aggregation $\rightarrow$ colloids (nucleation) ,

V. H $\rightarrow$ dislocations and colloids ,

VI. F → dislocations and colloids ,

VII. Colloid growth (F – H) and dislocation climb (H – F) determined by net fluxes

VIII. F + halogen molecular centers → cation vacancies .

For application of results from α-radiation damage experiments with alkaline-earth fluorides, alkali, and alkaline-earth chlorides, Exarhos (1982) observed the following: the larger the cation size and mass, the lower was the probability of observing localized color centers, but the larger was the change in lattice constant.

This phenomenon would happen at high doses (as seen in plutonium storage containers) when there is an enhanced disorder of the heavier (larger) cations, which would be accompanied by a decrease in F-center concentration. Deposited energy from the α particles might be directed toward disordering the cation sublattice rather than to the formation of localized color centers. Color centers initially might be created, but thermal relaxation or recombination processes in the heavier chlorides might preclude observing them. It is also possible at such high α doses for the F centers to recombine, thereby reducing the radiation damage to the NaCl crystal (Newton and Hay 1980, Newton and Hay 1979).

For aged salts, interstitial helium in its atomic form might possibly combine with the F and M centers to completely annihilate these defects (Wardle 1975). The probability of generating substitutional species during α-particle bombardment at doses above saturation is expected to lead to the replacement of a large number of lattice vacancies with substitutional ions. These substitutional ions are expected to serve in some sense as partial restoration of the lattice order (Wardle 1975).

At radiation doses comparable to the plutonium storage, a decrease in radiation damage with dose is likely. This decrease occurs because the radiation damage production decreases with increasing radiation dose as a result of the precipitation of halogen molecular centers near dislocation lines. In other words, when the amount of damage increases, the probability of F-center formation, as well as an H-center formation, will be captured by the same damage form (halogen molecular centers) increases, resulting in annihilation of a just-created F-H pair (Seinen, 1994). This annihilation is supposed to reduce the production efficiency and the crystal will become saturated more rapidly.

Experimental results published in the early 1950s suggest that NaCl crystals exposed to x-rays contain 0.1 and 0.6 “free” chlorine atoms per vacancy pair or one “free” chlorine atom for each F center (Hacskaylo et al. 1953). This finding was based on experiments with thin films of NaCl deposited on transmission electron microscopy (TEM) grids and electrons irradiated in an electron microscope at 5–40 keV range (Medlin and Howitt, 1994). A low G value of ~ 2 to 5 pairs/100 eV for initial production of F-H pairs in alkali halides at room temperature was reported (Hobbs 1979, Medlin and Howitt 1994, Sonder and Sibley 1971). However, because most of these rapidly recombine, researchers suggest that the G value near

room temperature for stable F-H production in NaCl is ~0.032 pairs/100 eV (Hobbs 1979, Medlin and Howitt 1994, Itoh and Tanimura 1990). This G value is similar to one reported for various radiation sources at high doses for MSRE fluoride salts of 0.02 F_2 molecules/100 eV (Williams et al. 1996).

Medlin and Howitt (1994) observed experimentally that, even though the chlorine-signal decay in TEM experiments varies with electron energy (as expected from Bethe's stopping equation), the absolute decay rate was an order of magnitude lower with a G value of 0.0013 Cl/100 eV.

Egerton and associates (1987) used the decay of halogen atom to measure the diffusion of H center to the surface of the specimen, resulting in the loss (sputtering) of the halogen atom. This result suggests that multiple displacements are necessary to remove the chlorine atom from the foil, thus effectively lowering the observed cross section.

According to the experimental model suggested by Medlin and Howitt (1994), the ionization damage and not the diffusion controls the decomposition rate (i.e., formation and recombination of F-H center pairs). Important to the PuO_2 storage situation is that the chemical decomposition of NaCl slows down with increased sample thickness (Egerton et al. 1987).

Other literature reports suggest that the diffusion process (for example, the diffusion of H centers) is the rate-limiting factor (Egerton et al. 1987, Szymonski et al. 1997, Szymonski et al. 1996, and Townsend et al. 1976). This model helps predict the rates of decomposition as a function of specimen thickness and irradiation dose (Egerton et al. 1987, Medlin and Howitt 1994). For bulk crystals at high temperatures, after the initial creation of F and H centers, the H centers can migrate inside the crystal, arrive at the surface, and eventually decay to the halogen atom adsorbed on the crystal surface, which evaporates out (Szymonski et al. 1997). Szymonski believes this process to be the thermal component of desorption, which is controlled by the diffusion process. Experimentally, the jump distance associated with these events in NaCl is 15 nm. This number is based on predictions from specimens of different thickness, along with the measurement of chlorine signal decay from a 120-nm-thick NaCl sample irradiated with the 30-keV electrons (Medlin and Howitt 1994). Egerton and colleagues (1987) showed loss of chlorine in NaCl to decrease with the dose rate for a given dose. This finding can be of significance to the storage of PuO_2 materials.

Experimentally, Szymonski and coworkers (1990) observed the sputtering of halogen atoms in NaCl when the salt was irradiated with 5-keV Ar^+). For foil irradiated KCl in a microscope at room temperature and at extremely high doses of 10^{10} Gy, Hobbs (1975) observed that highly strained halogen molecular inclusion (highly compressed halogen gas or liquid bubbles) occupy 2% of the lattice volume.

Several researchers reported observing sputtering of chlorine, sodium, and sodium chloride from the surface of NaCl crystals during exposure to low-energy electrons in a highly evacuated environment (Elliott and Townsend 1971, Paparazzo et al. 1997, Tokutaka et al. 1970). However, other investigators, who exposed NaCl to high doses of fast electrons or to γ radiation while NaCl was sealed within evacuated ampoules, could not detect chlorine upon opening the irradiated ampoules by sensitive mass spectrometry (MS) (Didyk et al. 1971, Compton et al. 1972). Researchers offered no explanations for the apparent differences between the two types of experiments, but these differences could be an artifact of the experiment itself (i.e., there could be in the later experiment possible adsorption and loss of the chlorine to either the walls of ampoules or to the inlet of the MS itself).

Were chlorine gas actually to be observed sputtering, the condition would offer a possible mechanism for chlorine gas release caused by radiolysis of the salt by ^{241}Pu-emitted β particles. Even with other forms of radiation, sputtering does provide such a possible mechanism for the release of some chlorine into the gas phase in the material containers. Most of the chlorine formed as a result of radiation damage will remain within the crystal lattice. Sputtering is extremely rare and only soft β particles from ^{241}Pu could contribute to the generation of chlorine gas through this process. So far, sputtering has only been observed for irradiated *foils* of alkali halides (particularly at elevated temperatures); it has not been reported for crystals irradiated in bulk outside the microscope.

Empirical data collected so far at LANL does not suggest any stress corrosion or cracking from the generation of chlorine gas or HCl in the plutonium storage containers. However, more experimental data on the contents of these containers (such as the identity of the salts, G values, percentage of radiation damage, chlorine, or HCl generation over time) might prove to be extremely helpful in substantiating theoretical predictions of radiation damage.

Formation and Detection of Metal Colloids and Chloride Species

The mechanism for forming sodium metal colloids under certain conditions (mobile molecular centers and above-room temperature) leads to the appearance of chlorine inclusions or bubbles (Hobbs 1975, Lidiard 1978, Seinen 1994). The inclusions or bubbles then become even less effective as annihilation sites for the F centers (Hughes and Pooley 1971, Lidiard 1978).

The formation of colloidal aggregates of sodium provides additional stability to radiation defects in NaCl (Burns and Williams 1955). However, the nucleation sites for the colloids are not homogeneously distributed near the dislocation lines, impurities, or charge-compensating defects (Hughes and Jain 1979). The colloidal alkali metal particles (formed by the coming together of F centers) have diameters in the 10–100 nm range (Lidiard 1978, Seinen 1994). Natarajan and colleagues (1989) conducted thermally stimulated luminescence (TSL) studies on ^{239}Pu- and ^{241}Am-doped NaCl and KCl. They found the TSL glow curves for both the α-irradiated salts to be similar.

Based on the irradiation experiments with CaF_2, even at high doses, α-irradiated samples gave higher intensity for F centers than for the colloidal particles. Exarhos (1982) observed the opposite situation for CaF_2 electron irradiated at comparably high doses: the spectral results are similar to NaCl, in which the formation of colloidal particles predominates. Based on the experimental data from α-irradiated NaCl crystals, the chance of F centers recombining with H centers at such high doses is very likely (Newton and Hay 1980, Newton and Hay 1979). When rock salts were exposed to high doses (~10^9 Gy) of γ radiation, the concentration of chlorine measured was only 0.1 ppm (Jockwer and Mönig 1989). *In situ* exposure of rock salts to ^{60}Co at comparably high doses resulted in 0.4 μmol neutral chlorine atoms per gram of salt (Gies et al. 1994).

The formation of chloride ion in salts is often accompanied by an increase in molecular hydrogen concentration because the Cl^- ions act as scavengers for the hydroxyl radicals (as shown in reactions 26–29 on p. 26 and water (Panno and Soo 1984). This would reduce the yield of chloride concentration over time (Lewis and Warren 1989). Because the generation of hydrogen is one of the possible reactions for sodium colloid with water, the corrosive gas yields would be even lower. One also has to take into account that only parts of the gases produced will end up in the gas phase of the void volume.

Hydrochloric acid might be formed if both hydrogen (also formed by the reaction of alkali colloids with water molecules) and molecular chlorine are released from the salt into the gas phase and react (Jenks and Baes 1980). These phenomena might play a significant role in plutonium storage containers. Hydrochloric acid might also be formed even when trace amounts of moisture are present (Kelm and Bohnert 1996). The concentration of HCl is probably going to be very low in plutonium storage containers because one of the main products of radiolysis of water is going to be reformation of water itself. The concentration of various reactive species that can lead to the formation of HCl is also expected to be very low. LANL researchers have demonstrated that HCl is either absent or present at extremely low-gas concentrations in the headspace gas over Hanford material (aged 13-years-old PuO_2 with chloride impurities).

Headspace gas analysis samples from Hanford site did indicate the presence of HCl at very low levels; but a quantitative estimate could not be made. Experimentally, in most cases, both HCl and chlorine might not even be observed in the gas phase because of the complexities of the system. Moreover, the detection of chlorine and HCl would be extremely difficult because these gases are extremely aggressive. To detect these gases, even at relatively high concentrations, an optimization of experimental setup and analytical methods will be required (Compton et al. 1972, Didyk et al. 1971, Jenks and Bopp 1977, Levy 1983, Palut et al. 1993, Panno and Soo 1984). The permeability, the porosity, the diffusivity, and the mechanism of transport will determine the gas transport in the material.

The permeability and porosity are not affected by the mineralogical content of the material (Brewitz and Mönig 1992). We suggest small-scale laboratory experiments to study the various effects of radiation damage on salts in material containers and to optimize the detection system for determining HCl and chlorine gas.

Effect of Impurities

One of the possible roles of impurities is to act as H-center traps (Soppe et al. 1994). The effect of impurities on radiation damage is rather complicated and largely depends both on the kinds and forms of impurities that are present. F-center production by MeV protons and α particles is less sensitive to the presence of electron-capturing impurities, such as Tl, than for x-ray irradiation (Thompson et al. 1978). These impurities suppress F-center growth.

The results from crystals being deliberately doped with impurities show a larger amount of radiation damage than natural crystals containing impurities (Soppe et al. 1994). This increase in radiation damage is because, for doped crystals, the impurities are present in the host lattice and appreciably affect the production and aggregation of F and H centers, while, for the natural salt, the impurities are precipitated on grain boundaries (Soppe et al. 1994). In many cases (as discussed below), the higher the impurity levels, the greater the radiation damage. Therefore, for nominally pure samples, the type impurities and their concentrations need to be known accurately to readily predict the formation of dislocation loops and colloids.

The formation and quantities of colloidal alkali metal and atomic chlorine depends on the impurity levels because of the strong relationship between the number of dislocation loops and the impurity concentration (Soppe et al. 1994, Seinen 1994). Reducing the mobility of interstitials through trapping leads to an enhanced growth of colloids (Soppe et al. 1994). If additional oxygen is present, the amount of chlorine formed (along with colloidal centers) might increase (Compton 1957, Didyk et al. 1971, Hughes and Jain 1979, Seinen 1994, and Tsal' and Didyk 1970).

The presence of excess amounts of calcium and sulfur suppress the colloid formation (Gies et al. 1994, Levy 1983, Levy et al. 1983). According to the review article by Hobbs (1975), at room temperature large concentrations (1000 ppm or higher) of divalent impurity ions (such as Ca^{2+} and Sr^{2+}) can suppress observable halogen interstitial aggregation, possibly because the accompanying charge-compensating cation vacancies are effective interstitial traps. The presence of divalent impurity ions (such as Ca^{2+}, Pb^{2+}, and Sr^{2+}) can raise the temperature at which the aggregation of radiation-induced defects in alkali halides takes place (Kotomin et al. 1994).

Presence of these impurities at 800°C for alkali-halide melts have an opposite effect; i.e., they lead to an increased radiolytic decomposition of the substance caused by removal of halogen in the gas phase (Makarov et al. 1982, Pikaev et al. 1982). Sodium chloride crystals doped

with various impurities (such as potassium, lithium, fluorine, bromine) and mixed dopant KBF_4 were irradiated with 1.3-MeV electrons at 0.02 to 2.5×10^6 Gy/h, with doses varying between 5×10^7 Gy and 1.5×10^9 Gy (Seinen 1994, Seinen et al. 1994b). The impurity levels were selected to be at levels seen in natural rock salts. The irradiation temperature was varied in the 20°C–150°C range.

The difference in the radiation damage behavior of lithium- and potassium-doped crystals was significant. The amount of damage (precipitated sodium and chlorine) in lithium-doped crystals saturated at approximately 1%. However, in potassium-doped crystals the radiation damage did not saturate even at 1.5×10^9 Gy (Seinen 1994). For the latter case, Seinen (1994) observed radiation damage of up to 10% and suggested the likelihood of this phenomenon being related to the dose rate.

This radiation damage may have resulted because, when the crystals reached a damage level of 1% in potassium-doped crystal, another type of sodium colloid with completely different properties began to form. This phenomenon was observed only at high doses of 0.3×10^9 Gy and 1.5×10^9 Gy, with a dose rate between 0.5 and 2.5×10^6 Gy/h. Therefore, the dose rate and total received dose are possible factors governing the radiation damage, so extreme caution must be exercised in making predictions for nuclear waste based on laboratory experiments (Seinen 1994). The dose rate in plutonium storage containers is several orders of magnitude less at 2.2 Gy/s or 7920 Gy/h.

The effect of impurities on chlorine generation would be less pronounced for the actual plutonium oxide material because the radiation damage from the primary source of radiation is α particles. The products in this case will be less prone to attack by impurities, particularly those that act as scavengers. Impurity concentrations are already determined for select batches of representative samples, both before and after calcination, in containers from various DOE sites.

Effect of Temperature

The temperature inside the plutonium storage containers would be greatly affected by several factors, including the following:

- quantity of material,
- maximum power of PuO_2 in container,
- density of material,
- thermal conductivity for the particles,
- fill gas, and
- anticipated storage in a three-dimensional array.

Knight and Steinke (1997) found that other factors affecting the thermal conductivity are porosity of the grains, particle size of the oxide, individual thermal conductivities of the particle, and cover gas. The temperature inside the can would also be affected by the temperature of various objects and structures surrounding the container, changes in specific power, etc. The Knight and Steinke paper provides an in-depth study of thermal analysis.

Garibov (1983) demonstrated that if water molecules were adsorbed on the surface of plutonium oxide, increasing the temperature would lead to a greater desorption rate of water from the oxide surface, thereby inhibiting effective energy transfer to adsorbed molecules. The hydrogen yield G (hydrogen) strongly depends on LET increasing by a factor of 3 to 4 from γ radiolysis to α radiolysis (Bibler 1974, Bibler 1975, Burns and Sims 1981, Spinks and Wood 1990, TRUPACT II SARP 1994).

Kalinichenko and colleagues (1988) compared the G (hydrogen) values for water and water vapor under the influence of α irradiation from ^{244}Cm and ^{238}Pu. The yield was 1.05 molecules/100 eV for water and 5.8 ± 0.3 molecules/100 eV for water vapor. As the hydrogen pressures increase, the energy deposition in the gas phase will also increase; at a few atmospheres of pressure, equilibrium between the rate of hydrogen formation and water recombination will take place (Gray and Simonson 1984). The higher the temperature, the higher is the G (hydrogen) and the more rapidly the equilibrium is achieved. A series of theoretical evaluations and experiments presently being carried out at LANL are studying the issues related to hydrogen generation in plutonium storage containers. These experiments will be discussed in detail elsewhere in this paper.

According to most of the literature reports, at temperatures below 150°C the radiation defects in salts are expected to increase with temperature. According to Akram and associates (1992), at higher temperatures the F centers become more mobile and are more easily trapped to form colloids. When the temperature is raised, the stability of sodium colloid is reduced. The F centers migrate again ("evaporation"), forming Na^+ ions and further react with interstitial Cl_2^- (H-center pairs) to give Cl^- ions. The result of this migration is the progressive annealing of defects. An increase in temperature can also result in the reduction in yields of hydrogen and chlorine, particularly when reactions 30–32 (p. 27) become key factors (Lewis and Warren 1989).

Defect aggregation appears to reach a maximum at a distinct temperature for a particular dose rate (Levy 1991, Levy 1983, Levy et al. 1983, Levy et al. 1981). However, if the dose rate is decreased, there is a shift of this maximum toward lower temperatures (Kotomin et al. 1994, Seinen 1994). The radiation defect formation is equivalent to energy storage in the salt, which increases with dose (Rothfuchs et al. 1995, Weber and Ewing 1997).

Long-term exposure to high levels of radiation in plutonium storage containers is expected to heat up the material, including both the actinide and nonactinide fractions. According to many literature reports, when the salts are exposed to a high-integrated dose at >50°C, the colloid

formation starts to saturate (Clark and Crawford 1973, Levy 1991, Levy 1983, Levy et al. 1983, Levy et al. 1981, Rothfuchs et al. 1995). Thermally activated annealing of radiation defects in the oxide phase may take place at higher temperatures, thereby reducing the yield of both chlorine and colloidal alkali metals in the material.

When the temperatures exceed 150°C, the amount of energy stored in the salts is reported to be negligible because thermally activated annealing becomes a key factor (Jenks and Bopp 1977, Pederson et al. 1986). At these and higher temperatures, the colloidal sodium can be dispersed again to F centers (Lidiard 1978). A large number of reports suggest a two-step annealing process at higher temperatures for salts irradiated at room temperature (Catlow et al. 1980, Hobbs 1975, Hughes and Jain 1979).

Experiments with ^{239}Pu- and ^{241}Am-doped NaCl and KCl salts at dose rates of 10^3 Gy indicated a partial thermal annealing of radiation-induced F centers at 77°C and 137°C in NaCl and 127°C in KCl (Natarajan et al. 1989). Natarajan and colleagues observed total annealing of α-induced F and M centers at 187°C in NaCl and 177°C in KCl, possibly as a result of an interstitial halogen atom (hole) recombining with an F-center electron at these temperatures. Hughes (1978) suggested a similar two-step annealing model under various irradiation conditions, including when NaCl was irradiated with 350-MeV protons at an integrated dose of 10^7 Gy.

Levy (1991) observed an interesting aspect of temperature dependence: below 150°C the radiation-induced color center and colloid particle bands in natural and synthetic rock salt changed very little after irradiation. However, at higher temperatures the decay that occurs after irradiation was shown to spread with increasing temperature. These experiments also suggest that to determine the kinetics of radiation-induced processes, one must make measurements during irradiation.

Hughes and Jain (1979) irradiated sodium chloride crystals at room temperature to a dose of 0.1 to 1×10^7 Gy and then heated the crystals to higher temperatures. They observed that annealing took place in steps as the temperatures increased; F, M, R centers annealed out at 150°C to 200°C and were converted at least partly into colloids. When the temperatures exceeded 250°C, the colloids disappeared by taking part in the F-center-interstitial recombination process. Other reports show the same findings (i.e., partial annealing of the salt takes place between 200°C and 250°C and complete annealing at 300°C to 400°C).

When alkali halides, such as NaCl, are irradiated at temperatures in which F centers are known to be mobile enough to form colloids (i.e., ≥50°C in NaCl), then the growth of colloids could be significant (Levy 1991, Lidiard 1998, Panno and Soo 1984). Once the nucleation takes place, a colloid becomes an effective sink for mobile F centers. The growth of colloids competes with the dynamic F-center-interstitial recombination, which at room temperature and lower than room temperature restricts the saturation level of irradiation-induced defects to approximately 0.1% (Hughes and Jain, 1979).

Some researchers observed a total defect concentration of 1% at high temperatures. Vacancy-molecule complexes that are created, together with the dislocation loops, are believed to play an important role in annealing of metal colloids, with the colloids annealing at ~220°C and the dislocation loops disappearing at ~350°C (Catlow et al. 1980, Hobbs 1975). The possible models for colloid growth at high temperatures and high-irradiation doses are discussed in review articles by several authors (Hughes and Jain 1979, Levy 1991, and Lidiard 1998).

Increased sputtering may occur in materials that contain ^{241}Pu in which the release of chlorine as gas from radiation-damaged salts could possibly take place. At 150°C, Szymonski and coworkers (1996) obtained a sputtering yield of 8 molecules per keV electron for chlorine and sodium atoms desorbed from very thin film of NaCl films (film thickness 30º–1000ºA), when these were exposed to 1-keV electrons. These researchers observed that at 150°C even the bulk H center has a chance to reach the surface and evaporate, thus contributing to the desorption. Szymonski and colleagues (1995) reviewed the electron-stimulated desorption for alkali halides and found that for several alkali halides (including KCl) a significant part of the neutral halogen atoms are ejected with nonthermal energies (i.e., energies of the order of 0.1 to 1.0 eV) (Szymonski et al. 1997, Szymonski et al. 1995).

The remaining part of the halogen atoms and all alkali atoms evaporate from the surface with the Maxwellian spectrum of kinetic energies. Temperature-dependent studies revealed that if alkali-halide surfaces were subjected to prolonged electron bombardment at temperatures higher than room temperatures, the apparent enrichment of the alkali component caused by halogen sputtering vanishes with increasing temperature (Townsend et al. 1976). This phenomenon happens at a rate related to thermal evaporation properties of the alkali halide. Electron-stimulated desorption occurs as a result of activating only the halogen sublattice, whereas the alkali component is neutralized and evaporated thermally from the surface (Poradzisz et al. 1988, Szymonski et al. 1995, Szymonski et al. 1990). It is possible that the presence of oxygen in compressed-powder samples will reduce thermal evaporation of sodium, as compared to a single crystal of NaCl (Szymonski et al. 1990).

The observed shift to higher temperatures and doses for colloid formation under α irradiation may be caused by helium introduced as the α particles come to rest. If helium is trapped in F centers, then higher doses and temperatures may be required to produce colloids.

Experiments with radiolysis of alkali-halide melts of NaCl and KCl at temperatures of ≥800°C, showed an almost complete reconstruction of the original substance, even at levels of radical reactions (Makarov et al. 1982, Pikaev et al. 1982). As a result, the radiation chemical yield of chlorine (following γ radiolysis of melts of chloride) was very low at <0.001 molecules/100 eV (Pikaev et al. 1982).

The set of reactions responsible for the recovery in alkali melts is possible in plutonium storage containers, but only to a limited extent because in alkali melts the nature of solvents

(ionic liquid) and temperatures are different (Pikaev et al. 1982). To recombine any free fluorine formed as a result of radiolysis, the salts from the MSRE project were reheated periodically at >150°C, but they stayed well below the melting point of salts ~450°C (Notz 1988). This annealing was deemed ineffective in later years (Williams et al. 1996).

Hobbs suggested that, at higher temperatures, the halogen gas may diffuse out of the inclusions, perhaps annihilating the alkali metal colloids or diffusing out of the crystal, thus leaving behind empty cavities that can lower surface energy by faceting. A process such as this can explain the observed cubic cavities in foils heavily irradiated in the microscope (heated considerably as a result) and in crystals annealed following irradiation (Hobbs 1975). Several factors would govern the temperature inside the plutonium storage containers for both the solid material and the gas phase (as discussed at the beginning of this "Effect of Temperature" section).

Based on data from theoretical models for predicting temperature in both the PuO_2 and the gas phase in British Nuclear Fuels Laboratory (BNFL) containers at Rocky Flats Environmental Technology Site, it is likely that temperatures in the individual containers will not exceed 100°C in isolated pure PuO_2 containers (Knight and Steinke 1997). These researchers reported, depending on the density of the pure PuO_2 material in BNFL containers, an average theoretical temperature range of 72.5°C to 86.5°C for isolated containers with specific power of 3 W/kg and 115.7°C to 142.3°C respectively for materials with specific power of 6 W/kg. The temperature in impure oxides will even be lower.

Generally, materials with very high salt content have lower plutonium and americium concentrations. Therefore, α dose and the resulting radiation damage to the salts in these materials is also lower. However, in storage facilities that have a large number of containers placed in one room, the temperature of materials would be greater than 150°C.

Researchers need to take extreme caution when they are extrapolating data on theoretical maximum temperatures because—as was mentioned earlier—several factors play a key role in governing the maximum temperature. Generally, the gas temperature in void volume above the material is lower than the solid phase. For actual material in plutonium storage containers in which the plutonium oxide is not pure, the power as is expected to be lower, along with the temperature.

LANL researchers measured temperatures of actual PuO_2 for nine representative Hanford Site containers used for gas analysis. The temperature of these materials was generally <50°C (with one exception), primarily because of the low wattage and the small quantity of materials (plutonium and americium), <1500 g. Excluding one sample, the range of specific power in these containers was low, 0.32–5.08 W.

One sample had a very specific power of 9.97 W. The average temperature of the material inside this container was 126°C. The higher temperature in this isolated container is believed

to be caused by a very high americium content of 43.62 g. The total volume of this container is only 52.8 in^3, and the total plutonium and americium content is 678 g. Therefore, as expected, because of the high specific activity of ^{241}Am, materials with high americium content will generally have higher temperatures.

It should be noted that in storage the containers will not be isolated but in a three-dimensional array. In such a matrix, some container temperatures are estimated to reach 250°C or higher. Experiments to determine the exact identity of the salts and to determine the effects of temperatures and annealing on actual material might prove to be very useful. Some current work at Savannah River Site indicates that the chemistry and the form of mixed stored materials can change over the years as a result of interactions between the species induced by radiation.

Annealing Effect and Stored Energy

Annealing of crystal defects leads to the liberation of accumulated energy. As expected, experiments involving a two-step annealing process indicate that energy is also released at the two annealing temperatures. Hobbs (1975) reports the energy released in the second step to be smaller. However, Spitsyn and coworkers (1981) obtained contrary results in experiments. For halites exposed to γ irradiation at very high doses of 10^6, 10^7, and 10^8 Gy, only a small portion of the energy was liberated at 20°C to 110°C, but then the major portion of energy was released at higher temperatures of 170°C to 320°C.

The temperatures at which the accumulated energy is liberated or thermal annealing takes place are independent of the dose absorbed by the salt (up to 10^8 Gy). However, the efficacy of the liberated energy increases with absorbed dose. Therefore, to prevent the liberation of accumulated energy, the temperature in the salts should not exceed the lower limit of the high-temperature release interval (i.e., 170°C) (Spitsyn et al. 1981). Weber and Ewing (1997) discuss the temperature dependence of stored-energy accumulation and defect-recovery kinetics.

In the literature, a limited number of systematic studies appear on radiation-induced stored energy, despite extensive research on primary defects in alkali halides. Because different research groups have used different experimental setups that lead to variations in experimental results, it is difficult to make a direct comparison of stored energy (Soppe et al. 1994). Soppe and associates observed an S-shape curve if stored energy is plotted as a function of dose. However, the saturation value decreases with increasing temperature. The amount of energy stored in the first stage (i.e., the colloid nucleation stage) in a dose range of 0 to 2.5×10^6 Gy, is very small and mainly caused by dislocations.

The colloid formation as a function of temperature is a bell-shaped curve; i.e., for a given dose rate and total dose, the fraction of colloids has a maximum at a certain temperature (Soppe et al. 1994). For doses lower than 5×10^6 Gy (i.e., early stages of colloid growth), a clear dose-

rate is dependent on the stored energy (Levy 1983, Soppe et al. 1994). However, for higher doses the situation is less clear.

Significant amounts of chlorine gas and colloidal sodium are formed from 2.5×10^6 Gy to 0.1×10^9 Gy. In the second stage, the stored energy increases exponentially with increasing dose. For doses in the 0.01×10^9 Gy range and for dose rates between 0.01 to 2.5×10^6 Gy/h, the optimum temperature for colloid formation is between 100°C to 150°C. The third stage involves doses $< 0.1 \times 10^9$ Gy; the stored energy then levels off with increasing doses and reaches a saturation value at 0.5×10^9 Gy. The reported saturation values for stored energy vary by nearly a factor of ten and range from 50 to 365 J/g. Maximum stored energy is also slightly dependent on dose and dose rate (Soppe et al. 1994).

For higher dose rates of $\sim 0.01 \times 10^9$ Gy/h, the optimum temperature for colloid formation was shifted to 175°C and 250°C. Also, an increase in maximum stored energy (or colloid fraction) occurs with decreasing dose rate, but only in the colloid growth stage. For example, in pure NaCl irradiated to a total dose 1×10^9 Gy, a colloid fraction of 1 mol % is reported at a dose rate of 1×10^6 Gy/h, which increases to about 10 mol % for a dose rate of 1×10^5 Gy/h. This means that decreasing the dose rate by one order of magnitude leads to an increase of colloid fraction by 10% (Soppe et al. 1994). On the other hand, the theoretical saturation value of colloid fraction (and thus the stored energy) is not higher for smaller dose rates (Soppe et al. 1994).

Levy and Kierstead (1983) have suggested that on a unit dose basis, low dose rates are more effective than high dose rates in producing sodium colloids. It should be mentioned that the dose-rate effect is not well established and is often contradictory. Ideally, small-scale experiments on dose-rate effects might prove to be extremely useful, but they are not recommended at this stage because of the very small amount of HCl or chlorine that is known to form as a result of radiolysis in actual high-salt containers at LANL.

For electron irradiation doses above 5×10^7 Gy, depending on the analytical method used to measure the stored energy per sodium atom (i.e., optical absorption or differential scanning calorimetry), a value of 6.2 ± 1 eV or 5.3 ± 0.5 eV has been suggested (Seinen 1994, Seinen et al. 1994). The stored energy is a measure of damage (F, M, R colloidal centers) produced by irradiation. Other authors have suggested a theoretical value of 5 eV and an experimental value of 4.25 eV (Hughes 1978, Jenks and Bopp 1977).

During the storage of radioactive material, there is always a chance of local temperature rise. A rise in temperature above 170°C can lead to an instantaneous liberation of accumulated energy and, consequently, an additional temperature rise (Spitsyn et al. 1981). As mentioned, major thermal annealing or the liberation of accumulated energy in salts takes place above 170°C and can result in hazardous consequences (Spitsyn et al. 1981).

Experimentally, Spitzyn and coworkers (1981) showed that if halite samples were irradiated at 200°C to 220°C, there is a complete absence of low-temperature release of energy and the intensity of high-temperature release interval was 10–15 times lower. During irradiation at higher temperatures, the radiation defects are annealed in the process of irradiation itself. Similar phenomena were also observed for rock salts doped with 0.1 mol % K (Seinen 1994, Seinen et al. 1994a). Therefore, keeping the temperature in the storage high at 200°C to 220°C for halides hinders the process of energy accumulation in the halide. Seinen also found that an unplanned temperature increase as a result of liberation of accumulated energy can be prevented by keeping the temperature in the waste container within the limits of a high-temperature release interval.

In the case of containers in storage throughout the DOE complex, LANL researchers believe that, even though the material in individual containers is probably going to be maintained at lower temperatures (<100°C), as long as there is no sudden increase in temperature by a few hundred degrees Celsius, the issue of rapid release of stored energy will not be a factor. This conclusion seems likely because the amount of chloride salts present in these containers is small (less than 10% after calcination). Also, the maximum radiation damage predicted in these materials will be <10 %, and, therefore, the amount of energy stored in these salts will not be large enough to make a significant impact on the integrity of the container. In fact, materials with higher salt contents will have lesser quantity of radionuclides present; and, therefore, the radiation damage (and stored energy) will be smaller too.

Levy (1991) observed that if plutonium storage containers are maintained at temperatures ≥150°C, which becomes more likely in storage facilities that contain large number of cans, annealing of radiation damage to salts will proceed, lessening the steady state of radiation damage to a few percent. This temperature level also reduces the chances of an accidental release of large quantities of stored energy. If the temperatures were high, they would also contribute to the removal of water adsorbed on the PuO_2 particles, and the chances of significant hydrogen generation and over-pressurization would also be affected (Spitsyn et al. 1981).

Results from temperature measurements of both pure and impure PuO_2 in actual material are discussed in the earlier section on effects of temperature. These measurements and gas-phase analysis can be very beneficial in making predictions that pertain to radiation damage in salts and hydrogen generation.

Extensive practical experience with plutonium pyrochemical salt materials has not indicated any evidence of significant stored energy in these materials, even after they have aged for many years. This practical experience is confirmed by two recent calorimetric investigations of aged plutonium pyrochemical salts.

1. Researchers in the Material Identification and Surveillance (MIS) program at LANL (Morales 1999) ran 114 differential gravimetric analysis/differential scanning

calorimetry (DTA/DSC) measurements on 33 aged samples from RFETS and Hanford. A number of these samples contained chloride, in one case above 20 wt %. Researchers observed no significant exotherms attributable to stored energy release.

2. This result is corroborated by a hazards investigation of pyrochemical salts that had been stored for many years at RFETS (Eberlein, 1998a,b). DTA investigations of these materials showed no significant exotherms, a result that assisted in downgrading the hazard index from high to low. Thus, the technical literature, recent measurements, and considerable practical experience with plutonium pyrochemical salts support the conclusion that stored energy does not represent a significant issue for safe storage of chloride-containing plutonium materials.

Soppe and coworkers suggested that one potential risk of the radiolysis process in salts (such as NaCl) is a sudden back-reaction of metallic sodium and gaseous chlorine. If the back-reaction exceeds a certain percolation threshold, a large amount of energy could be released (Soppe et al. 1994). Based on certain assumptions in a salt repository, the critical concentration is estimated to be equivalent to a colloid fraction of 12 mol %. If this critical concentration is reached, a spontaneous back-reaction will take place, releasing a large amount of energy in a small volume (i.e., causing an expansion of the salt crystals).

More studies are recommended to attain more realistic values for a percolation threshold. In the plutonium storage containers, taking all the mentioned factors into account, it is highly unlikely that the concentration levels for metallic sodium and chlorine will exceed 12 mol % to cause an explosive reaction.

Effect of Particle Size

The particle size is the most important factor in material depletion caused by radiolysis of a substance surrounding a plutonium particle. If the sizes are on the order of atomic dimensions and there is the usual excess of material, the material would never be depleted. If the particle sizes were greater than 30 μm, the depletion times would not be much less than a few months because the plutonium then absorbs an appreciable fraction of radiation (Kazanjian 1976). Based on the specific activities, materials around the ^{238}Pu oxide particle should deplete 300 times faster than that of ^{239}Pu oxide particle. However, experimental results do not necessarily agree with these predictions (Kazanjian 1976). For α particles, maximum damage occurred to the crystal lattice at the end of particle range because the energy deposited is maximum at that position (Wardle 1975).

Energy straggling causes the increased depth of coloration at high doses. Luntz and colleagues (1977) suggested that F-center concentration does not follow *dE/dx* and instead profile shapes and magnitudes can be accounted for in terms of the concept of ion infratrack. The infratrack is characterized by high-energy density and dose rate, surrounded by a region of low-energy density.

In rock salts, higher gas yields are understandably obtained for smaller grain-size particles because for smaller salt particles the radiation penetration before energy loss is more complete (Akram et al. 1992). In electron-irradiated, smaller-grain evaporated samples (similar to the oxides in material containers) with a large surface-to-volume ratio, Hobbs (1975) suggested that irradiation leads to halogen desorption that produces alkali-rich surface layers, which can react with the residual gases present.

The amount of energy absorbed by a particle depends on the size of the particle and its density. The calculated range of ^{238}Pu (in PuO_2 with maximum theoretical density of 11.4 g/cm^3) was 11 μm (Bibler 1979). Another independent set of calculations (as shown in Appendix A) also indicates a range of 11 μm for PuO_2. Turcotte (1976) suggested a range of ~13 μm.

A very simple model suggests that it can be assumed that the outer 11–12-μm shell of the PuO_2 particle contains radionuclides from which many α particles can escape with substantial residual energy (as discussed later). It is assumed for the present purposes that 100% of the α energy, or any other form of radiation present in the plutonium storage containers, is transferred to the salts. (See Appendix B, "Particle Size Effects in PuO_2.") This effect will be diminished with increasing PuO_2 particle size. It should be noted that Appendices A and B are oversimplified models, which give the bounding conditions and the worst-case scenario for α-energy loss in the salts.

The calculated ranges of 5-MeV α particles, ignoring channeling effects (in NaCl and KCl), are approximately 28 and 34 μm, respectively (Potetyunko and Shipatov 1976). Researchers performed tests to determine the particle size, by both particle number and volume, in selected containers from each DOE site. The mean spherical equivalent by particle volume in these materials when calcined at 950°C is reported to be 28–99 μm. The mean spherical equivalent generally increases after calcination at high temperatures.

The distribution of particle size varies from one container to another. Data at LANL from various DOE sites also suggest that the majority of the energy of the particles is going to be deposited within the PuO_2 itself, except when the plutonium particles are present on the surface, because the larger particles carry most of the activity. Appendix A, B, and C discuss the alpha energy that escapes from PuO_2 particles. A slight variation in density occurs in different PuO_2 materials in various plutonium storage containers. Therefore, the range of α particles also will be different.

Turcotte (1976) suggested, based on rigorous calculations, that 1/4 α flux will be coming out from an infinitely thick α source (i.e., in cases where particle thickness or diameter is >α range). At the surface of the plutonium oxide particle, the probability of α escape is exactly one-half, depending on whether the path is into or away from the particle. Turcotte also suggested that within the source and at a depth just greater than the range, the escape

probability is zero. Therefore, the average escape probability of α particles for the full thickness of plutonium particle will be one-fourth.

Other studies have shown that a significant fraction of the oxide-particle-size distribution will exceed 3–5 μm, after calcination at 950°C, depending upon the method by which the oxide was formed (Haschke and Ricketts 1995, Machuron-Mandard and Madic 1996). Therefore, it is clear that at least to some extent plutonium self-absorption will limit the α dose that can be delivered to adjacent phases.

Results from TRIM Monte Carlo Computer Simulations

Recently, to calculate the radiation damage, stopping power, and range, computer simulations based on Monte Carlo methods were used at LANL to simulate slowing down of 5.15-MeV α particles (average α energy of PuO_2) in UO_2, ThO_2, H_2O and in the various salts. This review discusses those results briefly.

We used a computer simulation program called the Stopping and Range of Ions in Matter (SRIM) 2000, version 9 (International Business Machines [IBM] Corporation, 1998). The SRIM is a group of programs that calculate, among other things, the stopping power and range of ions (10 eV–2 GeV/amu) into matter, using quantum mechanical treatment of ion-atom collisions. The source code with full explanations of its physics and calculations can be found elsewhere (Ziegler et al. 1985).

The Monte Carlo program, Transport of Ions in Matter (TRIM), is an extremely comprehensive program included with the SRIM package. The TRIM program can be applied for multilayer targets with multi-atomic compositions. It calculates the three-dimensional distribution of ions and also all kinetic phenomena associated with the energy loss: target damage, sputtering, ionization, and phonon production. All target atom cascades are followed in detail. This simulation program follows a large number of individual ion or particle "histories" in a target. Each history begins with a given energy, position, and direction (Biersack and Haggmark 1980, Ziegler 1977-1985).

On the TRIM code, the history (distribution of energy, range referred to as "longitudinal range," and stopping power, etc.) of 1000 α particles with a starting energy of 5.15 MeV were followed at various angles and in different targets. See Appendix C, "TRIM Particle Size Analysis," Table C-1; and the text tables that present TRIM Monte Carlo Computer Simulation Results—Table 4, "Theoretical Range for Uranium Oxide (Density of PuO_2) at Various Angles"; Table 5, "Theoretical Range of Various Oxide Materials"; Table 6, "Theoretical Range for Water"; and Table 7, "Theoretical Range for Salts."

Ideally for this project, we were most interested in the range of α particles in PuO_2. But, because the periodic table in the TRIM only goes up to uranium (Z = 92), estimates of

radiation damage are made based on UO_2 assuming it has the same density as pure PuO_2, i.e., 11.46 g/cm^3 (Table 4).

The various factors that influence stopping power and range are discussed in Appendix A. Because uranium and plutonium have similar atomic and mass numbers and the key player, density, is already accounted for, at LANL we estimated that stopping power and range calculated using the TRIM program can easily be extrapolated to PuO_2 to an accuracy of within ±5%.

TRIM Monte Carlo Computer Simulation Results

Table 4. Theoretical Range for Uranium Oxide (Density of PuO_2) at Various Angles

Ion Type: He (4.003 amu)
Ion Energy: 5.15 MeV
Number of Ions Analyzed : 999

Target Layer	Depth (μm)	Density (g/cm^3)	Longitudinal Range (μm)	Longitudinal Straggle	Ion Angle, (Degrees)
UO_2	20	11.46	12.8	6385°A	0
UO_2	20	11.46	12	6702°A	20
UO_2	20	11.46	9.04	9424°A	45
UO_2	20	11.46	6.37	1.07 mm	60
UO_2	20	11.46	1.11	8327°A	89

The computer simulation results in Table 5 indicate that the lower the density, the higher the range. For comparison purposes, we computed results from UO_2 and ThO_2 with their actual densities. Based on these computer simulations, ~12.8 μm is estimated for 5.15-MeV α particles travelling in pure PuO_2 at an angle of incidence of 0°.

It is evident from Table 4 that the angular distribution of the salts will be very critical to the radiation damage. Therefore, only a small portion of the salt particles that are present within the range of α and at the correct angles will undergo extensive radiation damage.

Table 5. Theoretical Range of Various Oxide Materials

Ion Type: He (4.003 amu)
Ion Energy: 5.15 MeV
Number of Ions Analyzed: 999

Target Layer	Depth (μm)	Density (g/cm^3)	Longitudinal Range (μm)	Longitudinal Straggle (°A)	Ion Angle (Degrees)
ThO_2	20	10*	14	6809	0
ThO_2	20	11.46	12.2	5942	0
PaO_2	20	10.46*	13.8	6835	0
UO_2	20	10.97*	13.3	6670	0

*Actual density of the material

In Appendix C, the range calculated by TRIM was converted to the units of mg/cm^2. This conversion is generally done to annul the effects of density that can vary with temperature and pressure and will effect the linear range in μm. In Appendix C, the tabulations estimate the uncertainty associated with the range of PuO_2 calculated in Table 4. We accomplished these tabulations by comparing the trend in stopping power in mg/cm^2 for a series of five elements, using either the true or assumed densities and/or the true Z (90, 91, 92, 93, and 94), and then using Z = 92 and the true densities for 93 and 94.

The density reflects the diminishing cell size and outweighs the alternate reversing of molecular weights because of isotope stability. The increase in stopping power was about 0.6 mg/cm^2 addition for two atomic number increases. It was noted that the uranium value and just the increasing densities for neptunium and plutonium, the total stopping power stayed nearly constant. Similarly, for ThO_2, using its Z = 90 and widely differing densities, the same stopping power in mg/cm^2 was almost the same, with the depth differing appropriately. Even in Appendix C (Fig. C-1), it seemed difficult to explain why the stopping power would suddenly halt at about 14.6 or 14.7 mg/cm^2, when it had been rising from ThO_2 to UO_2.

This issue is currently being further investigated, but if this value keeps increasing at the same rate from uranium to plutonium, the range of 12.8 μm for PuO_2 could be slightly lower. But still it seems highly unlikely that the TRIM calculations for the range are more than ±0.5 μm.

The range of water calculated in Table 6 using the TRIM program, agrees very well with the literature values (Spinks and Wood, 1990). The TRIM program suggests a value for 5.15-MeV α particles in water as 37.9 μm that is in good agreement with the experimentally determined literature value of 38.9 μm calculated for 5.3-MeV α particles emitted by ^{210}Po (Spinks and Wood, 1990).

Table 6. Theoretical Range for Water

Ion Type: He (4.003 amu)
Ion Energy: 5.15 MeV
Number of Ions Analyzed: 999

Target Layer	Depth (μm)	Density (g/cm^3)	Longitudinal Range (μm)	Longitudinal Straggle (°A)	Ion Angle (Degrees)
H_2O (Liquid)	40	1	37.9	3841	0

As shown in Table 7, the range of 5.15-MeV α particles in the various salts is supposed to be 25.1–30.6 μm respectively. These results account for the differences in densities and stopping power of the various salts. Salts crystals rapidly become damaged under ion bombardment, and there can be up to 5% density change in the surface region of NaCl crystals alone.

Table 7. Theoretical Range for Salts

Ion Type: He (4.003 amu)
Ion Energy: 5.15 MeV
Number of Ions Analyzed: 999

Target Layer	Depth (μm)	Density, (g/cm^3)*	Longitudinal Range (μm)	Longitudinal Straggle (°A)	Ion Angle (Degrees)
NaCl	40	2.165	26.3	5611	0
KCl	40	1.98	30.6	4370	0
$CaCl_2$	40	2.152	28.4	5841	0
$MgCl_2$	40	2.325	25.1	4749	0

* Salt crystals rapidly become damaged under ion bombardment, and there can be up to 5% density change in the surface region of NaCl crystals alone. TRIM calculations for NaCl account for these density changes.

The TRIM calculations for NaCl account for these density changes. Computer simulations were carried out for mixed-layered targets made up of UO_2 (assumed density of 11.46 g/cm^3) and NaCl. The goal of these calculations was to simulate the conditions for radiation damage to the salts present either as a layer on the outer shell of PuO_2 or immediately adjacent to the oxide. We analyzed the energy deposition patterns for α particles emitted from the outer shell

of the PuO_2. Alpha particles of 5.15 MeV energy were again used. The LET patterns were very similar to the ones suggested in Appendix A and by Sunder (1998). Also, as expected, most energy was deposited in the salts at the end of the particle range.

As stated earlier, if the PuO_2 particle radius exceeds the stopping distance of the α particles, an increasing number of α particles will be completely self-absorbed. However, because the PuO_2 was calcined at temperatures above the melting points of possible alkali and alkaline earth halides, once the oxides are allowed to cool, it is not certain whether the salts are segregated or are either adsorbed or absorbed around the particles.

Indeed, one possible explanation for lower radiation damage in these salts is a result of larger salt particles in the materials. In other words, when the particle size of the salts in calcined material exceeds the α-particle range, one observes only surface radiation effects in these salts. Generally, the MIS data at LANL on spherical equivalent mean particle-size analysis (insoluble particles) and mean spherical equivalent by volume, for oxide from Hanford and RFETS materials calcined at 950°C also support these findings (Mason et al. 1999). But, for smaller-sized particle, the chlorine gas is evolved more readily (Panno and Soo 1984).

Electron microscopy experiments are suggested to be carried out on the PuO_2-salt mixtures after melting the halides to help answer the key question of where the salts exist with respect to the PuO_2 particles.

Corrosion and Stress-Corrosion Cracking

Corrosive gases (e.g., Cl_2, Cl_2^-, HCl, H_2S) can reduce the lifetime of material containers (Pikaev et al. 1982, Levy et al. 1981). Corrosion of steel by HCl also generates additional gases, such as hydrogen (Jockwer and Mönig 1993, Gommlich et al. 1995). For this HCL gas production to take place, the corrosive gas molecules need only to circulate from the point of production in the oxide to the gas phase and then to a reactive surface, a process expected to take no more than a few seconds (Van Konynenburg et al. 1996). This condition makes detecting HCl in field tests impossible.

Panno and Soo (1984) suggested that, depending on the irradiation conditions, the pH of the brine solutions that results from the presence of water around irradiated rock salts changes (i.e., the higher the temperature of the salt during irradiation, the higher the pH of the resulting brine). The high alkalinity of the solutions made from irradiated salts was explained to be caused by NaOH formation. However, the pH and total base values stabilize for annealing temperatures >120ºC. This effect was the result of thermal degradation of bicarbonates and carbonates and CO_2 and the dissolution of acidic gas constituents such as HCl and SO_2 at high annealing temperatures (Panno and Soo, 1984). Reda and coworkers (1986) observed that when saturated solutions of brine (NaCl and $MgCl_2$) are exposed to high-level γ radiation fields, a significant increase in the rate of corrosion of Type 1018 mild

steel occurs because corrosive oxidizing radiolysis products form. The type of corrosion that happens is intergranular corrosion (instead of uniform corrosion observed for nonirradiated brines).

In the plutonium storage containers (which are made of Type-300-series stainless steel), pit corrosion and stress corrosion might be more prominent; and, therefore, the concept of uniform corrosion rates might not be relevant. However, if pit corrosion and/or stress corrosion occurs, the corrosion is not an issue because there is not enough water to corrode the container.

In Type-304 stainless-steel containers, the rate of failure by localized corrosion depends on the following factors:

- critical potential, which is dependent on the container material;
- temperature and anionic concentrations (Cl^-, NO_3^- etc.); and
- corrosion potential, which is determined by the container material and environmental variables (O_2, H_2O_2, pH, and temperature) (Osada and Muraoka 1993, Walton et al. 1994).

Radiolysis of the available moisture and air in an unsaturated environment in the material containers will create transient species that can significantly change the pH and/or Eh of the available moisture (Piepho et al. 1989). These changes can influence rates of container corrosion.

In the absence of water, corrosion and stress corrosion and cracking will not be an issue until high temperatures such as 400°C are reached. Otherwise, dry HCl will not cause corrosion. Secondly, gas-induced failure per se is not an issue (Kolman and Butt 1997). This lack of gas-induced failure is also supported by experimental observations at LANL showing little pressurization after 13 years. They include handling large quantities of these materials and analyzing headspace gas.

However, the adsorption/condensation of water from a gas onto a surface is an issue. Above 100°C, there probably will not be a problem with corrosion or stress corrosion and cracking because there will not be any moisture for adsorption/condensation (Kolman and Butt 1997). Kolman and Butt conducted a detailed investigation on potential mechanisms of corrosion and stress-corrosion cracking failure of 3013 storage containers made of 316 stainless steel. Experiments are presently underway at LANL to address these issues.

Piepho and colleagues (1989) have suggested, in conducting long-term modeling calculations, that a transient chemical kinetics model may be more exact than an equilibrium model. This model is preferable because, in reality, the environmental conditions in the material (such as temperature, radiation rate, and available moisture) are all expected to change over long-time

storage periods. In addition, the production rates of various species and chemical rate constants are basic required data and must be known accurately if extrapolation to long-term storage conditions is to be accurate. Therefore, to ensure that the theoretical predictions are valid, these researchers suggest that laboratory experiments be carried out especially on previously electrorefined salts.

Summary

This review of the extensive literature on radiation effects focuses on chloride salts. The goal is to provide a basis for estimating the magnitude of such effects on chloride salts that can accompany plutonium oxide (PuO_2) into storage. It was noted that literature data comprise largely radiation effects produced with low-LET (linear energy transfer) radiation, not high-LET alpha radiation that will originate from the plutonium.

Evaluation of the available data as applied to the contents of plutonium storage containers, yields the following.

- In the extreme case when PuO_2 and chloride salts are so intimately mixed that the total radiation energy is deposited in the salt, over a storage period of 50 years, the total energy from 5 kg of weapons-grade PuO_2 is about 10^9 Gy. (This finding clearly exaggerates the salt damage because much of the plutonium alpha activity will be expended within the PuO_2 particles themselves.)
- Radiation-induced defects within the salt lead to energy storage, which can be released continuously because temperatures up to 250°C to 300°C are estimated in a vault that contains an extended matrix of PuO_2 storage containers. The DTA/DSC data from the MIS program for high-salt materials in storage do not show any signs of release of energy in these containers.
- Saturation of radiation damage occurs at 0.5×10^9 Gy (Soppe et al. 1994), resulting in a damage range of 0.1 to 1 mol %. In a worst-case scenario, the amount of radiation damage at such high doses is not expected to exceed 10 mol %.
- Physically, radiation damage is restricted to shallow depths because of the short α penetration (range); the total would be diminished with increased particle size of the salt. The fraction of salts that accompany the PuO_2 and would be converted into metallic alkali colloids and molecular chlorine centers is limited.
- The majority of species that result from radiation damage remain within the salt. Their escape from the salt particles is a very inefficient process.
- Straining of salts during the blending process can possibly lead to enhanced F-center- and colloid-formation rates, as suggested by Levy and Kierstead (1984) and needs to be further explored. (The straining issue is not discussed in this report.)

- The concentration of the species that can lead to the formation of HCl is expected to be very low. Hence, the concentration of HCl will be correspondingly low. This prediction was confirmed by analysis of headspace gas over stored materials that contain PuO_2 and chlorides. After 13-year sealed storage, only trace levels of HCl and no can corrosion were observed.
- Because of the paucity of data dealing with α radiation and chloride salts, experiments with PuO_2/chloride salt mixtures need to be begun to collect such data. These experiments are needed in spite of the fact that observation at LANL with cans that contained PuO_2 plus chloride salts showed neither corrosion nor pressurization after 13 years of sealed storage.

Acknowledgements

The author wishes to express great appreciation to the following consultants: Lee Hyder, presently with CDI Corporation, Albuquerque (Savannah River Technology Center, retired); Robert A. Penneman (LANL, retired); and the following individuals at LANL: Gary Eller (Materials Science and Processing Group), Lynn Foster (Nuclear Materials Management, Control, and Accountability Group), Stan Kosiewicz (Environmental Technology Group), and Craig Leasure (Nuclear Weapons Materials and Manufacturing Program Office). These people made invaluable suggestions, took the time to participate in numerous discussions, and reviewed the manuscript. Initial suggestions by Dani Misel (University of Notre Dame Radiation Laboratory) and Sinisa Djordjevic (Benchmark Environmental) were extremely helpful. The author also wishes to express appreciation to David Horrell (LANL Nuclear Weapons Materials and Manufacturing Program Office) and Steve McKee (LANL Pit-Disassembly and Surveillance Technology Group) for their invaluable support. Finally, the author thanks Linda K. Wood (LANL Communication Arts and Services Group) for her editorial support.

References

1. Aguilar, M., F. Jaque, and F. Agulló-López, "Computer Simulation of Coloring Curves in Alkali Halides by Using a Heterogeneous Nucleation Model," *Radiat. Eff.* **61**, 215, 1982.

2. Aguilar, M., F. Jaque, and F. Agulló-López, "M-Center Growth in Alkali Halides: Computer Simulation," *Radiat. Eff.* **72**, 193 (1983).

3. Akram, N., M. T. Gaudez, P. Toulhoat, J. Mönig, and J. M. Palut, "Multi-parameter Study of Gas Generation Induced by Radiolysis of Rock Salt in Radioactive Waste Repositories," in *Disposal of Radioactive Waste. Gas Generation and Release from Radioactive Waste Repositories,* Proceedings of a Workshop Organized by NEA in Cooperation with ANDRA (Aix-en-Provence, September 23-26, 1991), p. 130.

4. Aleksandrov, A. B., A. L. Gusev, and N. G. Petrik, "Energy Aspects of the Radiolysis of Water on the Surface of Alkali Halide Crystals," *Russ. J. Phys. Chem.* **61(1)**, 102 (1987).

5. Allen, A. O., C. J. Hochanadel, J. A. Ghormley, and T. W. Davis, "Decomposition of Water and Aqueous Solutions Under Mixed Fast Neutrons and Gamma Irradiation," *J. Phys. Chem.* **56**, 575 (1952).

6. Bergsma, J., R. B. Helmholdt, and R. J. Heijboer, "Radiation Dose Deposition and Colloid Formation in a Rock Salt Waste Repository," *Nucl. Technol.* **71**, 597, (1985).

7. Bibler, N. E., "Radiolysis of 0.4-M Sulfuric Acid Solutions with Fission Fragments from Dissolved Californium-252. Estimated Yields of Radical and Molecular Products that Escape Reactions in Fission Fragment Tracks," *J. Phys. Chem.* **79(19)**, 1991 (1975).

8. Bibler, N. E., "Curium-244 α Radiolysis of Nitric Acid. Oxygen Production from Direct Radiolysis of Nitrate Ions," *J. Phys. Chem.* **78(3)**, 211 (1974).

9. Bibler, N. E., "Gas Production from Alpha Radiolysis of Concrete Containing TRU Incinerator Ash, Progress Report 2, August 1, 1978–November 30, 1978," E. I. DuPont de Nemours and Company, Savannah River Laboratory report DPST-78-150-2 (1979).

10. Bibler, N. E., and E. G. Orebaugh, "Radiolytic Gas Production from Tritiated Waste Forms, Gamma and Alpha Radiolysis Studies," E. I. DuPont de Nemours and Company, Savannah River Site report DP-1459 (1977).

11. Biersack, J. P., and L. G. Haggmark, "A Monte Carlo Computer Program for the Transport of Energetic Ions in Amorphous Targets," *Nucl. Instrum. Methods* **174**, 257 (1980).

12. Billington, D. S., and J. H. Crawford, *Radiation Damage in Solids* (Princeton University Press, Princeton, New Jersey), 1961.

13. Bird, J. R., A. Rose, and R. W. T. Wilkins, "Proton Decoration of Halite Crystals," *Aust. J. Phys.* **34**, 529 (1981).

14. Bjergbakke, E., Z. D. DragniC, K. Sehested, and I. G. DragamiC, "Radiolytic Products in Waters." Part II: "Computer Simulation of Some Radiolytic Processes in Nature," *Radiochim. Acta* **48,** 73 (1989).

15. Brewitz, W., and J. Mönig, "Sources and Migration Pathways of Gases in Rock Salt with Respect to High-Level Waste Disposal," *Disposal of Radioactive Waste. Gas Generation and Release from Radioactive Waste Repositories* (Proceedings of a workshop organized by NEA in Cooperation with ANDRA (Aix-en-Provence, September 23-26, 1991), p. 41.

16. Büppelmann, K., J. I. Kim, and Ch. Lierse, "The Redox Behavior of Plutonium in Saline Solutions under Radiolysis Effects," *Radiochim. Acta* **44/45(1)**, 65 (1988).

17. Burns, W. G., and H. E. Sims, "Effect of Radiation Type in Water Radiolysis," *J. Chem. Soc., Faraday Trans. 1* **77 (11)**, 2803 (1981).

18. Burns, W. G., and T. F. Williams, "Chemical Effects Associated with 'Colour Centers' in Alkali Halides," *Nature* **175**, 1043 (1955).

19. Catlow, C. R. A., K. M. Diller, and L. W. Hobbs, "Irradiation-Induced Defects in Alkali-Halide Crystals," *Philos. Mag. A* **42(2)**, 123 (1980).

20. Chadderton, L. T., *Radiation Damage in Crystals* (Methuen, London, 1965).

21. Clark, C. D., and J. H. Crawford, "The Interaction of Colour Centres and Dislocations," *Adv. Phys.* **22(2)**, 117 (1973).

22. Compton, R. N., V. E. Anderson, A. Carter, C. D. Cooper, J. T. Cox, F. J. Davis, W. R. Garrett, D. R. Nelson, P. W. Reinhardt, H. C. Schweinler, J. A. Stockdale, and J. F. Wilson, "Electron and Ion Collision Physics," *Health Physics Division Annual Progress Report for Period Ending July, 31, 1972,* Oak Ridge National Laboratory report ORNL-4811 (1972).

23. Compton, W. D., *Phys. Rev.* **107**, 1271 (1957).

24. "Criteria for Preparing and Packaging Plutonium Metals and Oxides for Long-Term Storage," DOE-STD-3013-96 (U.S. Department of Energy, Washington, DC, 1996).

25. den Hartog, H. W., and D. I. Vainshtein, "Explosive Phenomena in Heavily Irradiated NaCl," *Mater. Sci. Forum* **239-241**, 611 (1997).

26. Didyk, R. I., Yu V. Karavan, Z. V. Stasyuk, and N. A. Tsal', "Mass-Spectrometric Investigation of the Radiolysis of NaCl Crystals," *Sov. Phys. Solid State* **12(12)**, 2951 (1971).

27. Dreschhoff, G., and E. J. Zeller, "Effect of Space Charge on F Centers Near the Stopping Region of Monoenergetic Protons," *J. Appl. Phys.* **48 (11)**, 4544 (1977).

28. Eberlein, S. J., "Evaluation of Risks Associated with Electrorefining Salt—First Use (IDC 363) and Second Use (IDC 364)," Rocky Flats Environmental Technology Site report RS-090-031 (1998a).

29. Eberlein, S. J., "Evaluation of Risks Associated with Molten Salt – 8% Pulverized (IDC 408)," Rocky Flats Environmental Technology Site report (1998b).

30. Egerton, R. F., P. A. Cozier, and P. Rice, "Electron Energy-Loss Spectroscopy and Chemical Change," *Ultramicroscopy* **23,** 305 (1987).

31. Elliott, D. J., and P. D. Townsend, "Defect Formation and Sputtering of Alkali halides with Low-Energy Irradiation," *Philos. Mag.* **23,** 249 (1971).

32. Exarhos, G. J., "Spectroscopic Studies of α-Induced Radiation Damage in Divalent Metal Fluorides," *J. Phys. Chem.* **86,** 4020 (1982).

33. Fukasawa, T., Ch. Lierse, and J. I. Kim, "Radiolytic Oxidation Behavior of Neptunium in Sodium Chloride Solutions," *J. Nucl. Sci. Technol.* **33(6)**, 486 (1996).

34. Garibov, A. A., "Water Radiolysis in the Presence of Oxide," in *Proceedings of the Fifth Tihany Symposium on Radiation Chemistry, 1982* (Akademiai Kiado, Budapest, Hungary, 1983), Vol. 1-2, p. 377.

35. Gies, H., A. García Celma, J. B. M. de Haas, L. Pederson, and T. Rothfuchs, "Radiation Defects and Energy Storage in Natural Polycrystalline Rock Salt. Results of an In-Situ Test in the Permian Rock Salt of Asse," in *Materials Research Society Symposium Proceedings,* A. Barkatt and R. A. V. Konynenburg, Eds., (Materials

Research Society, Pittsburgh, Pennsylvania, 1994), Vol. 333, *Scientific Basis for Nuclear Waste Management XVII,* p. 219.

36. Gommlich, G., N. Jockwer, J. Schneefuß, and S. Heusermann, "Direct Disposal of Spent Fuel in Rock Salt: Geochemical Effects and Gas Release," in *ICEM '95, Proceedings of the Fifth International Conference on Radioactive Waste Management and Environmental Remediation,* S. Slate, F. Feizollah, and J. Creer, Eds., (The American Society of Mechanical Engineers, New York, 1995), Vol. 1, *Cross-Cutting Issues and Management of High-Level Waste and Spent Fuel,* p. 783.

37. Gray, W. J., and S. A. Simonson, "Gamma and Alpha Radiolysis of Salt Brines," Pacific Northwest Laboratory report PNL-SA-12746 (1984).

38. Hacskaylo, M., D. Otterson, and P. Schwed, "On the Presence of Free Chlorine in Sodium Chloride Crystals Containing Color Centers and Color Center Precursors," *J. Chem. Phys.* **21(9)**, 1434 (1953).

39. Haschke, J., "Does the Interaction of Plutonium Oxide with Water Pose a Potential Storage Hazard?" *The Actinide Research Quarterly of the Nuclear Materials Technology Division (*Los Alamos National Laboratory) **2,** 8 (summer 1996).

40. Haschke, J. M., and T. E. Ricketts, "Plutonium Dioxide Storage: Conditions for Preparation and Handling," Los Alamos National Laboratory report LA-12999-MS (1995).

41. Hobbs, L.W., "Point Defect Stabilization in Ionic Crystals at High Defect Concentrations," *J. Phys. (Paris) Colloq.* **C7**, C7-3, 1976.

42. Hobbs, L. W., "Transmission Electron Microscopy of Extended Defects in Alkali-Halide Crystals," in *Surface and Defect Properties of Solids,* M. W. Roberts and J. M. Thomas, Sr., Reporters (The Chemical Society, Burlington House, London, 1975), Vol. 4, p. 152.

43. Hobbs, L. W., "Radiation Effects in Analysis of Inorganic Specimens by TEM," in *Introduction to Analytical Electron Microscopy,* J. J. Hren, J. I. Goldstein, and D. C. Roy, Eds. (Plenum Press, New York, 1979), p. 437.

44. Hobbs, L. W., A. E. Hughes, and D. Pooley, "Nature of Interstitial Clusters in Alkali Halides," *Phys. Rev. Lett.* **28(4)**, 234 (1972).

45. Hollis, M. J., "Channeling of 1-MeV He^+ Ions in NaCl: Damage and Temperature Effects," *Phys. Rev. B, Solid State* **8(3)**, 931 (1973).

46. Hughes, A. E., and S. C. Jain, "Metal Colloids in Ionic Crystals," *Adv. Phys.* **28(6)**, 717 (1979).

47. Hughes, A. E., "Annealing of Irradiated Alkali Halides," *Comm. Solid State Phys.* **8(4)**, 83 (1978).

48. Hughes, A. E., and D. Pooley, "High-Dose Proton Irradiation of Alkali Halides," *J. Phys. C: Solid St. Phys.* **4**, 1963 (1971).

49. Hyder, L., J. Lloyd, and P. G. Eller, "Literature Search on Hydrogen/Oxygen Recombination and Generation in Plutonium Storage Environments," Los Alamos National Laboratory report LA-UR-98-4557 (1998).

50. Itoh, N., and K. Tanimura, "Formation of Interstitial-Vacancy Pairs by Electronic Excitation in Pure Ionic Crystals," *J. Phys. Chem. Solids* **51(7)**, 717 (1990).

51. Jain, U., and A. B. Lidiard, "Growth of Colloidal Centers in Irradiated Alkali Halides," *Philos. Mag.* **35(1)**, 245 (1977).

52. Jain, U., and A. B. Lidiard, "The Growth of Colloidal Centers in Irradiated Alkali Halides," *J. Phys. (Paris)* Colloq. **C7(12)**, 518 (1976).

53. Jenks, G. H., and C. F. Baes, Jr., "Review of Information on the Radiation Chemistry of Materials Around Waste Canister in Salt and Assessment of the Need for Additional Experimental Information," Oak Ridge National Laboratory report ORNL-5607 (1980).

54. Jenks, G. H., and C. D. Bopp, "Storage and Release of Radiation Energy in Salt in Radioactive Waste Repositories," Oak Ridge National Laboratory report ORNL-5058 (1977).

55. Jockwer, N., and J. Mönig, "Heat Induced Gas Generation in Rock Salt," in *Project on Effects of Gas in Underground Storage Facilities for Radioactive Waste (Pegasus Project),* B. Haijtink, T. McMenamin, Eds., (Proceedings of a Progress Meeting Held in Brussels, June 11–12, 1992), p. 50.

56. Jockwer, N., and J. Mönig, "Laboratory Investigation into the Radiolytic Gas Generation from Rock Salt. A Study Related to the Disposal of High-Level Radioactive Waste," in *Materials Research Society Symposium Proceedings,* W. Lutze and R. C. Ewing, Eds. (Materials Research Society, Pittsburgh, Pennsylvania, 1989), Vol. 127, *Scientific Basis for Nuclear Waste Management XII*, p. 913.

57. Johnson, E. R., *The Radiation-Induced Decomposition of Inorganic Molecular Ions* (Gordon and Breach, Science Publishers, Inc., New York), 1970.

58. Kalinichenko, B. S., V. G. Kulazhko, N. A. Kalashnikov, I. K. Shvetsov, and V. N. Serebryakov, "Application of Radiolysis of Water Vapor by Alpha-Radiation and Fission Fragments to Hydrogen Production," *Radiokhimiya (English Transl.)* **29(5)**, 647 (1988).

59. Kazanjian, A. R., "Radiolytic Gas Generation in Plutonium-Contaminated Waste Materials," Rockwell International, Atomics International Division, Rocky Flats Environmental Technology Site report RFP-2469 (1976).

60. Kazanjian, A. R., and A. K. Brown, "Radiation Chemistry of Materials Used in Plutonium Processing," The DOW Chemical Company, Rocky Flats Division, report RFP-1376 (1969).

61. Kelm, M., and E. Bohnert, "Radiolytic Compounds Formed by Dissolution of Irradiated NaCl and $MgCl_2 \cdot 6\ H_2O$ in Water," *Radiochim. Acta* **74**, 155 (1996).

62. Knight T. D., and R. G. Steinke, "Thermal Analyses of Plutonium Materials in British Nuclear Fuels, LTD., Containers," Los Alamos National Laboratory report LA-UR-97-1866 (1997).

63. Kolman, D. G., and D. P. Butt, "Potential Mechanism of Corrosion and Stress Corrosion Cracking Failure of 3013 Storage Containers Composed of 316 Stainless Steel," Los Alamos National Laboratory report LA-UR-97-4462 (1997).

64. Kotomin, E., M. Zaiser, and W. Soppe, "A Mesoscopic Approach to Radiation-Induced Defect Aggregation in Alkali Halides Stimulated by the Elastic Interaction of Mobile Frenkel Defects," *Philos. Mag, A* **70(2)**, 313 (1994).

65. Leasure, C. S., D. R. Horrell, and R. E. Mason, "Conditions and Results from Thermal Stabilization of Pure and Impure Plutonium Oxides for Long-Term Storage at Department of Energy Sites," Los Alamos National Laboratory report LA-UR-98-3526 (1998).

66. Levy, P. W., "Radiation Damage Studies on Non-Metals Utilizing Measurements Made During Irradiation," *J. Phys. Chem. Solids* **52(1),** 319 (1991).

67. Levy, P. W., "Radiation Damage Studies on Natural Rock Salt from Various Geological Localities of Interest to the Radioactive Waste Disposal Program," *Nucl. Technol.* **60**, 231 (1983).

68. Levy, P. W., and J. A. Kierstead, "Very Rough Preliminary Estimate of the Colloidal Sodium-Induced in Rock Salt by Radioactive Waste Cannister Radiation," in *Materials Research Society Symposium Proceedings,* G. L. McVay, Ed. (Materials Research Society, Pittsburgh, Pennsylvania, 1984), Vol. 26, *Scientific Basis for Nuclear Waste Management VII,* p. 727.

69. Levy, P. W., J. M. Loman, K. J. Swyler, and D. R. Dougherty, "Recent Studies on Radiation-Induced F-Center and Colloid Particle Formation in Synthetic NaCl and Natural Rock Salt," *Radiat. Eff.,* **72**, 303 (1983).

70. Levy, P. W., J. M. Loman, K. J. Swyler, and R. W. Klaffky, "Radiation Damage Studies on Synthetic NaCl Crystals and Natural Rock Salt for Radioactive Waste Disposal Applications," in *The Technology of High-Level Nuclear Waste Disposal 1,* P. L. Hofmann, Ed., U.S. Department of Energy, Oak Ridge, Tennessee Technical Information Center report DOE/TIC-4621 **(**1981), p. 135.

71. Lewis, M. A., D. F. Fischer, and L. J. Smith, "Salt-Occluded Zeolites as an Immobilization Matrix for Chloride Waste Salt," *J. Am. Ceram. Soc.* **76(11)**, 2826 (1993).

72. Lewis, M. A., and D. W. Warren, "Gas Generation from the Irradiation of Mortar," Argonne National Laboratory report DE89-013280 (1989).

73. Lidiard, A. B., "The Radiolysis of Alkali Halides—The Nucleation and Growth of Aggregates," *Z. Phys. Chem.* **206**, 219 (1998).

74. Lidiard, A. B., "The Radiolysis of the Alkali Halides," *Comm. Solid State Phys*. **8(4)**, 73 (1978).

75. Luntz, M., P. E. Thompson, R. B. Murray, and D. J. Whittle, "Ion Bombardment of Alkali Halides, III: Track-Effect Analysis of Measured Damage Profiles in KCl," *Radiat. Eff.* **31(2)**, 89 (1977).

76. Machuron-Mandard, X., and C. Madic, "Plutonium Dioxide Particle Properties as a Function of Calcination Temperature," *J. Alloys Compd.* **235**, 216 (1996).

77. Makarov, I. E., T. N. Zhukova, A. K. Pikaev, and V. I. Spitsyn, "Oxidizing Agents Produced by Radiolysis of Alkali-Metal Halide Melts," *Bull. Acad. Sci. USSR, Div. Chem. Sci. (Engl. Transl.)* **31(4)**, 662 (1982).

78. Mason, R. E., T. Allen, L. Morales, N. Rink, R. Hagan, D. Fry, L. Foster, E. Wilson, C. Martinez, M. Valdez, F. Hampel, O. Peterson, J. Rubin, and K. Hollis, "Materials

Identification and Surveillance: June 1999 Characterization Report," Los Alamos National Laboratory report LA-UR-99-3053 (1999).

79. McClain, W. C., and R. L. Bradshaw, "Status of Investigations of Salt Formations for Disposal of Highly Radioactive Power-Reactor Waste," *Nuclear Safety* **11**, 130 (1970).

80. Medlin, D. L., and D. G. Howitt, "The Analysis of Chlorine Signal Decay in Electron-Irradiated Sodium Chloride," *Radiat. Eff. Defects Solids* **128**, 221 (1994).

81. Molecke, M. A., and N. R. Sorensen, "Retrieval and Analysis of Simulated Defense HLW Package Experiments at the WIPP," in *Materials Research Society Symposium Proceedings,* W. Lutze and R. C. Ewing, Eds. (Materials Research Society, Pittsburgh, Pennsylvania, 1989), Vol. 127, *Scientific Basis for Nuclear Waste Management XII,* p. 653.

82. Morales, L. R., Los Alamos National Laboratory, unpublished results from the Materials Identification and Surveillance Program, 1999.

83. Morris, D. E., M. P. Eastman, P. G. Eller, L. E. McCurry, and D. E. Hobart, "Color Center Formation in Plutonium Electrorefining Residues," *Radiochim. Acta* **48**, 201 (1989).

84. Natarajan, V., T. K. Seshagiri, A. G. I. Dalvi, and M. D. Sastry, "Thermally Stimulated Luminescence Studies in Plutonium- and Americium-Doped Alkali Halides," *Nucl. Tracks Radiat. Meas.* **16(1)**, 37 (1989).

85. National Research Council, *Evaluation of the U.S. Department of Energy's Alternative for the Removal and Disposition of Molten Salt Reactor Experiment Fluoride Salts* (National Research Council, National Academy Press, Washington, DC, 1997).

86. Newton, C. S., R. B. Alexander, G. J. Clark, H. J. Hay, and P. B. Treacy, "Channeling Studies of Radiation Damage in Sodium Chloride Crystals," *Nucl. Instrum. Methods* **132**, 213 (1976).

87. Newton, C. S., and H. J. Hay, "A Two-Accelerator Facility and Its Use for Radiation Damage Studies in Alkali Halides," *Aust. J. Phys.* **33 (3)**, 549 (1980).

88. Newton, C. S., and H. J. Hay, "Helium Irradiation of Alkali Halides," *Radiat. Eff. Lett.* **43**, 211 (1979).

89. Notz, K. J., "Decommissioning of the Molten Salt Reactor Experiment. A Technical Evaluation," Oak Ridge National Laboratory report ORNL/RAP-17 (1988).

90. "Nuclear Materials—Plutonium-Bearing Solids—Calibration Technique for Calorimetric Assay," ANSI N 15.22-987 (American National Standards Institute, Inc., New York, 1987).

91. Osada, K., and S. Muraoka, "Corrosion of Stainless Steel for HLW Containers under Gamma Irradiation," in *Materials Research Society Symposium Proceedings,* C. G. Interrante and R. T. Pabalan, Eds. (Materials Research Society, Pittsburgh, Pennsylvania, 1993), Vol. 294, *Scientific Basis for Nuclear Waste Management XVI,* p. 317.

92. Palut, J. M., M. T. Gaudez, and N. Akram, "Gas Generation by Radiolysis of Rock Salt-HAW Project," *Project on Effects of Gas in Underground Storage Facilities for Radioactive Waste (Pegasus Project),* in Proceedings of a Progress Meeting held in Brussels, June 11–12, 1992, B. Haijtink and T. McMenamin, Eds., Vol. 64, p. 64.

93. Panno, S. V., and P. Soo, "Potential Effects of Gamma Irradiation on the Chemistry and Alkalinity of Brine in High-Level Nuclear Waste Repositories in Rock Salt," *Nucl. Technol.* **67**, 268 (1984).

94. Paparazzo, E., N. Zema, and L. Moretto, "Formation of Alkali Metal Layers at the Surface of Electron-Irradiated Alkali Halides," in *Materials Research Society Symposium Proceedings,* I. M. Robertson, G. S. Was, L. W. Hobbs, and T. D. de la Rubia, Eds. (Materials Research Society, Pittsburgh, Pennsylvania, 1997), Vol. 439, *Microstructure Evolution During Irradiation,* p. 651.

95. Pederson, L. R., W. J. Gray, F. N. Hodges, G. L. McVay, D. A. Moore, D. Rai, and J. A. Schramke, "FY 1984 Annual Report: Waste Package Environment Studies," Pacific Northwest Laboratory report PNL-5613 (1986).

96. Piepho, M. G., P. J. Turner, and P. W. Reimus, "The Importance of Variables and Parameters in Radiolytic Chemical Kinetics Modeling," in *Materials Research Society Symposium Proceedings,* W. Lutze and R. C. Ewing, Eds. (Materials Research Society, Pittsburgh, Pennsylvania, 1989), Vol. 127, *Scientific Basis for Nuclear Waste Management XII,* p. 905.

97. Pikaev, A. K., I. E. Makarov, and T. N. Zhukova, "Solvated Electron in Irradiated Melts of Alkaline Halides," *Radiat. Phys. Chem.* **19(5)**, 377 (1982).

98. Poradzisz, A., Z. Postawa, J. Rutkowski, and M. Szymonski, "Electronic Sputtering of Halides by Low-Energy Ion and Electron Bombardment," *Nucl. Instrum. Methods Phys. Res. Sect. B* **B33**, 830 (1988).

99. Potetyunko, G. N., and E. T. Shipatov, "Ionization Energy Losses and Range of Alpha Particles in Ionic Crystals," *At. Ènerg.* **40(4)**, 343 (1976).

100. Pretzel, F. E., "Radiation Damage to Alkali Halides and Other Simple Ionic Crystals," Los Alamos Scientific Laboratory report LA-3387-MS (1965).

101. Price, P. B., and J. C. Kelly, "Channeling of Protons and $^4He^+$ in Alkali Halides in Radiation-Damaged Conditions," *Phys. Rev. B* **17(11)**, 4237 (1978).

102. Reda, R. J., S. L. Akers, and J. L. Kelly, "Radiation-Enhanced Corrosion of Mild Steel," *Trans. Am. Nucl. Soc.* **53**, 224 (1986).

103. Roberts, F. P., R. P. Turcotte, and W. J. Weber, "Materials Characterization Center Workshop on the Irradiation Effects in Nuclear Waste Forms—Summary Report," Pacific Northwest Laboratory report PNL-3588 (1981).

104. Robinson, V. J., and M. R. Chandratillake, Chap. 14, in *Radiation Chemistry. Principles and Applications,* M. A. Farhataziz and J. Rodgers, Eds. (Wiley-VCH, New York, 1987).

105. Rothfuchs, T., N. Jockwer, J. Mönig, and K. Müller, "Designing and Testing of a High-Level Waste Disposal System at the Asse Salt Mine/Germany," in *ICEM '95, Proceedings of the Fifth International Conference on Radioactive Waste Management and Environmental Remediation,* S. Slate, F. Feizollah, and J. Creer, Eds. (The American Society of Mechanical Engineers, New York, 1995), Vol. 1, *Crosscutting Issues and Management of High-Level Waste and Spent Fuel,* p. 761.

106. Samuel, A. H., and J. L. Magee, "Theory of Radiation Chemistry II Track Effects in Radiolysis of Water," *J. Chem. Phys.* **21**, 1080 (1953).

107. Seinen, J., "Radiation Damage in NaCl. The Process of Colloid Formation," Ph.D. thesis, Rijksuniversiteit Groningen, Netherlands (1994).

108. Seinen, J., J. C. Groote, J. R. W. Weerkamp, and H. W. den Hartog, "Radiation Damage in NaCl. II. The Early Stage of F-Center Aggregation," *Phys. Rev. B* **50(14)**, 9787 (1994a).

109. Seinen, J., J. R. W. Weerkamp, J. C. Groote, and H. W. den Hartog, "Radiation Damage in NaCl. III. Melting Phenomena of Sodium Colloids," *Phys. Rev. B,* **50(14)**, 9793 (1994b).

110. Sonder, E., and W. A. Sibley, "Defect Creation by Radiation in Polar Crystals," in *Point Defects in Solids,* J. H. Crawford and A. Slifkin, Eds. (Plenum Press, London, 1971), p. 201.

111. Soppe, W. J., H. Donker, A. García Celma, and J. Prij, "Radiation-Induced Stored Energy in Rock Salt," *J. Nucl. Mater.* **217**, 1 (1994).

112. Spinks, J. W. T., and R. J. Wood, *An Introduction to Radiation Chemistry* (John Wiley & Sons, Inc., New York, 1990).

113. Spitsyn, V. I., V. D. Balukova, I. M. Kosareva, and S. A. Kabakchi, "Experimental Evaluation of Changes in Properties of Natural Minerals Under Irradiation," in *Scientific Basis for Nuclear Waste Management,* J. G. Moore, Ed. (Plenum Press, New York, 1981), Vol. 3, p. 429.

114. Sullivan, J. C., "Reactions of Plutonium Ions with the Products of Water Radiolysis," in *Plutonium Chemistry,* W. T. Carnall and G. R. Choppin, Eds. (American Chemical Society Symposium Series 216, Washington, DC, 1983), p. 241.

115. Sunder, S., "Calculation of Radiation Dose Rates in a Water Layer in Contact with Used CANDU UO_2 Fuel," *Nucl. Technol.* **122**, 211 (1998).

116. Szymonski, M., P. Czuba, T. Dohnalik, L. Jozefowski, A. Karawajczyk, J. Kolodziej, R. Lesniak, and Z. Postawa, "A Comparison of Ion- and Electron-Induced Sputtering of Single-Crystal Alkali Halides," *Nucl. Instrum. Methods Phys. Res. Sect. B* **B48**, 534 (1990).

117. Szymonski, M., J. Kolodziej, P. Czuba, and P. Korecki, "Stimulated Desorption from Bulk and Epitaxial Alkali Halides," *Mater. Sci. Forum* 239, 615 (1997).

118. Szymonski, M., J. Kolodziej, P. Czuba, P. Piatkowski, P. Korecki, Z. Postawa, and N. Itoh, "Thickness-Dependent Electron-Stimulated Desorption of Thin Epitaxial Films of Alkali Halides," *App. Surf. Sci.* **100(101)**, 102 (1996).

119. Szymonski, M., J. Kolodziej, Z. Postawa, P. Czuba, and P. Piatkowski, "Electron-Stimulated Desorption from Ionic Crystal Surfaces," *Prog. Surf. Sci.* **48(1-4)**, 83 (1995).

120. Thompson, P. E., M. Luntz, and R. B. Murray, "Ion Bombardment of Alkali Halides IV: Production of F-Centers by Positive Ions and X-rays in KCl and KCl(Tl)," *Radiat. Eff.* **35(3)**, 133 (1978).

121. Tokutaka, H., and M. Prutton, "The (100) Surfaces of Alkali Halides II," *Surf. Sci.* **21**, 233 (1970).

122. Toth, L. M., and L. K. Felker, "Fluorine Generation by Gamma Radiolysis of a Fluoride Salt Mixture," *Radiat. Eff. Defects Solids* **112**, 201 (1990).

123. Townsend, P. D., R. Browning, D. J. Garlant, J. C. Kelly, A. Mahjoobi, A. J. Michael, and M. Saidoh, "Sputtering Patterns and Defect Formation in Alkali Halides," *Radiat. Eff.* **30**, 55 (1976).

124. Trowbridge, L. D., S. H. Park, I. Remec, and J. P. Reiner, "Technical Basis of Selection of Trapping Technology for the MRSE Interim Vent and Trapping Project," Oak Ridge K-25 Site report K/TCD-1142 (1995).

125. "TRUPACT II Safety Analysis Report for the TRUPACT-II Shipping Package (SARP)," Nuclear Regulatory Commission Docket No. 9218 (1994).

126. Tsal', N. A., and R. I. Didyk, "On the Nature of X Centers in NaCl Crystals with Anionic Impurities," *Phys. Status Solidi* **40(1)**, 409 (1970).

127. Turcotte, R. P., "Alpha Radiation Damage in the Actinide Dioxides," in *Plutonium 1975 and other Actinides, 5th International Conference on Plutonium and Other Actinides* (Proceedings of conference in Baden Baden, September 10–13, 1975), H. Blank and R. Lindner, Eds. (American Elsevier Publishing Company, Inc., New York, 1976), p. 851.

128. Turner, J. E., *Atoms, Radiation, and Radiation Protection* (Pergamon Press Inc., New York, 1986).

129. Vainshtein, D. I., C. Altena, and H. W. den Hartog, "Evidence of Void Lattice Formation in Heavily Irradiated NaCl," *Mater. Sci. Forum* **239-241,** 607 (1997).

130. Van Konynenburg, R. A., D. H. Wood, R. H. Condit, and S. D. Shikany, "Bulging of Cans Containing Plutonium Residues: Summary Report," Lawrence Livermore National Laboratory report UCRL-ID-125115 (1996).

131. Walton, J. C., N. Sridhar, G. Cragnolino, T. Torng, and P. Nair, "An Approach to Analysis of High-Level Waste-Container Performance in an Unsaturated Repository Environment," in *Materials Research Society Symposium Proceedings,* A. Barkatt and R. A. V. Konynenburg, Eds. (Materials Research Society, Pittsburgh, Pennsylvania, 1994), Vol. 333, *Scientific Basis for Nuclear Waste Management XVII,* p. 863.

132. Wardle, M. W., "Color-Center and Radiation-Damage Effects in Alkali Halides Irradiated to High Particle Fluence," Ph.D. thesis, University of Delaware (1975).

133. Weber, W. J., and R. C. Ewing, "Radiation Effects in Glass Waste Forms for High-Level Waste and Plutonium Disposal," in *Materials Research Society Symposium Proceedings,* I. M. Robertson, G. S. Was, L. W. Hobbs, and T. D. de la Rubia, Eds. (Materials Research Society, Pittsburgh, Pennsylvania, 1997), Vol. 439, *Microstructure Evolution During Irradiation,* p. 607.

134. Weber, W. J., G. J. Exarhos, and L. M. Wang, "Temperature and Dose Dependence of Metal Colloid Production in Alpha-Irradiated CaF_2 Single Crystals," in *Materials Research Society Symposium Proceedings* (Materials Research Society, Pittsburgh, Pennsylvania, 1995), Vol. 373, *Microstructure of Irradiated Materials,* p. 311.

135. Weber, W. J., L. R. Pederson, W. J. Gray, and G. L. McVay, "Radiation Effects on Nuclear Waste Storage Materials," Pacific Northwest Laboratory report PNL-SA-11218 (1983).

136. Weber, W. J., L. R. Pederson, W. J. Gray, and G. L. McVay, "Radiation Effects on Nuclear Storage Materials," *Nucl. Instrum. Methods. Phys. Res. Sect. B* **B1**, 527 (1984).

137. Weber, W. J., J. W. Wald, and W. J. Gray, "Radiation Effects in Crystalline High-Level Nuclear Waste Solids," in *Scientific Basis for Nuclear Waste Management,* J. G. Moore, Ed. (Plenum Press, New York, 1981), Vol. 3, p. 441**.**

138. Williams, D. F., G. D. Del Cul, and L. M. Toth, "A Descriptive Model of the Molten Salt Reactor Experiment after Shutdown: Review of FY 1995 Progress," Oak Ridge National Laboratory report ORNL/TM-13142 (1996).

139. Wronkiewicz, D. J., "Radionuclide Decay Effects on Waste Glass Corrosion," in *Materials Research Society Symposium Proceedings,* A. Barkatt and R. A. V. Konynenburg, Eds. (Materials Research Society, Pittsburgh, Pennsylvania, 1994), Vol. 333, *Scientific Basis for Nuclear Waste Management XVII,* p. 83.

140. Ziegler, J. F., *The Stopping and Range of Ions in Matte (*Pergamon Press, New York, 1977-1985), Vols. 2–6.

141. Ziegler, J. F., J. P. Biersack, and U. Littmark, *The Stopping and Range of Ions in Solids* (Pergamon Press, New York, 1985).

Appendices

Appendix A

Radiation Dose Rates in Plutonium Oxide

Lee Hyder
Savannah River Technology Center, retired

The range of plutonium alpha particles (ca. 5 MeV) in plutonium oxide is just over 10 μm. Accordingly, in any substantial amount of this material, essentially all the radiation energy will be absorbed within the plutonium oxide itself. Even though there will be a substantial radiation field at the surface, this is only a small fraction of the total generated energy. The average radiation field within the plutonium oxide can be calculated by dividing the decay energy by the mass and applying the appropriate definitions. For plutonium oxide prepared from plutonium with a specific decay energy of 3 mW/g, the internal radiation field is just under 10,000 Gy/h or 1,000,000 rad/h. This is a substantial radiation field when compared to other sources of ionizing radiation, such as ^{60}Co irradiators.

Now consider the case in which a small amount of another material is introduced into the bed of plutonium oxide. This could be a halide salt, water, or interstitial gas. Consider a particle or layer of this material that is thin enough so that the alpha energies are not greatly degraded by passing through it. The flux of α particles will be identical to the average flux through the oxide bed. However, the energy deposition in the second phase, and therefore the radiation dose, will differ from that in the plutonium oxide because of the differences in densities and in the stopping powers of the two materials for alpha radiation. The relative stopping powers of Friedlander and colleagues (1981) discuss various materials for alpha radiation. These authors point out that their electron densities determine the stopping power of various media for alpha radiation. They provide graphs and equations for estimating this effect. Because the electron density per unit mass is higher for light elements than for plutonium, the energy deposition in these elements will be higher than in plutonium, and so the effective radiation dose will be higher. The stopping power of water is approximately three times that of plutonium oxide; and, therefore, the radiation energy deposited per unit mass (the radiation dose rate) is proportionately higher.

So long as this generalization holds (i.e., so long as the second material is a small fraction of the mass of the bed and is distributed as very small particles or thin layers), the radiation dose to this phase can be approximated by calculating the average radiation dose in the bed and multiplying by the difference in stopping powers between plutonium oxide and the material of interest. For larger particles and larger amounts of the second phase, the average dose rate will decrease, because the alpha flux will not be uniform through the material. For such cases, an accurate estimate of the energy deposition to the second phase would require a knowledge of the geometry and much more sophisticated calculation. However, for many

purposes it is enough to know that the dose rate to the second material will be of the order of the average dose rate in the package, or perhaps higher.

Reference

Friedlander, G., J. W. Kennedy, E. S. Macias, and J. M. Miller, *Nuclear and Radiochemistry,* 3rd ed. (John Wiley & Sons, New York, 1981).

Appendix B

Particle Size Effects in PuO_2

Stan Kosiewicz
Los Alamos National Laboratory
Environmental Science and Waste Technology Group

Alpha particles from ^{239}Pu have a very limited range in material because of their high linear energy transfer (LET). In dry air, the range is roughly 2 cm. In most organic materials, the range is approximately 50 μm. In halides, the range is ~30 μm. In PuO_2, the range is 11–12 μm. Appendix 3.6.7, attachment 1.0 of the TRUPACT-II SAR (1994), estimates the amount of alpha particle energy that escapes from spherical particles of a particular size distribution. That size distribution was determined for PuO_2 that was calcined at 1000°C. The intent of this attachment was to estimate the amount of energy that might be deposited from PuO_2 particles into organic material matrices with subsequent radiolysis.

Only the alpha particles emitted from the outer shell (11–12 μm) of larger PuO_2 particles can escape to the surface and be available for radiolysis. Alpha particles that are deeper than this are self-absorbed by the plutonium oxide. As an illustration, Table B-1 is reproduced from Table A1.2 of section 3.6.7, ATT. 1.0 the TRUPACT-II SAR.

Table B-1. Alpha Energy Escaping from $^{239}PuO_2$ Particles

Midpoint Particle Radius (μm)	Fraction of Alpha Energy Escaping
9.5	0.48
7.0	0.61
4.5	0.77
3.5	0.82
2.5	0.88
1.5	0.93
0.75	0.96
0.28	0.99

For the particle size distribution of the calcined PuO_2 used for the calculation, an estimate was made in the TRUPACT-II SAR that a maximum of 82% of the alpha-particle energy escaped from the plutonium oxide and was available to cause radiolytic degradation of the waste matrices.

If alkali-halide impurities were present in the Los Alamos plutonium oxide as separate particles or present as a very thin shell on the oxide, the alpha-particle irradiation available for interaction with them would be reduced by approximately 18%. For a scenario in which the impurities were homogeneously distributed throughout the oxide, 100% irradiation might be assumed. All the alpha-particle energy will be considered to be available for radiolytic degradation of alkali-halide impurities. This provides a margin of error (approximately 18%) that is conservative on the side of safety.

Reference

"TRUPACT II Safety Analysis Report for the TRUPACT-II Shipping Package (SARP)," Nuclear Regulatory Commission Docket No. 9218 (1994).

Appendix C

Table C-1. TRIM Particle-Size Analysis

Robert A. Penneman
LANL, retired

Z	mg/cm^2 MINUS 14	MOL WT	Z/A	X-RAY DENSITY	STOPPING DEPTH	mg/cm^2	DELTA	REMARKS
90 ThO_2	0	264.04	0.4015	10	14	14		TRUE Z
90 ThO_2	0	264.04		11.46	12.2	13.98	0	TRUE Z, PuO_2 DENSITY
91 PaO_2	0.43	263.1	0.4068	10.46	13.8	14.43	0.43	TRUE Z
92 UO_2	0.59	270.03	0.4	10.96	13.3	14.59	0.59	TRUE Z
93 NpO_2	0.66	269	0.4052	11.19	13.1	14.66	0.07	Z = 92
94 PuO_2	0.67	271	0.4059	11.46	12.8	14.67	0.01	Z = 92
92 UO_2	0.59	270.03	0.4	10.96	13.3	14.59		TRUE Z
92 UO_2	0.6			use ThO_2 at 10.0	14.6	14.6		low density
92 UO_2	0.64			use PaO_2 10.46	14	14.64		low density
92 UO_2	0.66			use NpO_2 11.19	13.1	14.66		high density
92 UO_2	0.67			use PuO_2 11.46	12.8	14.67		high density

Note: The second set of columns (lower columns) are all UO_2 @ different densities.

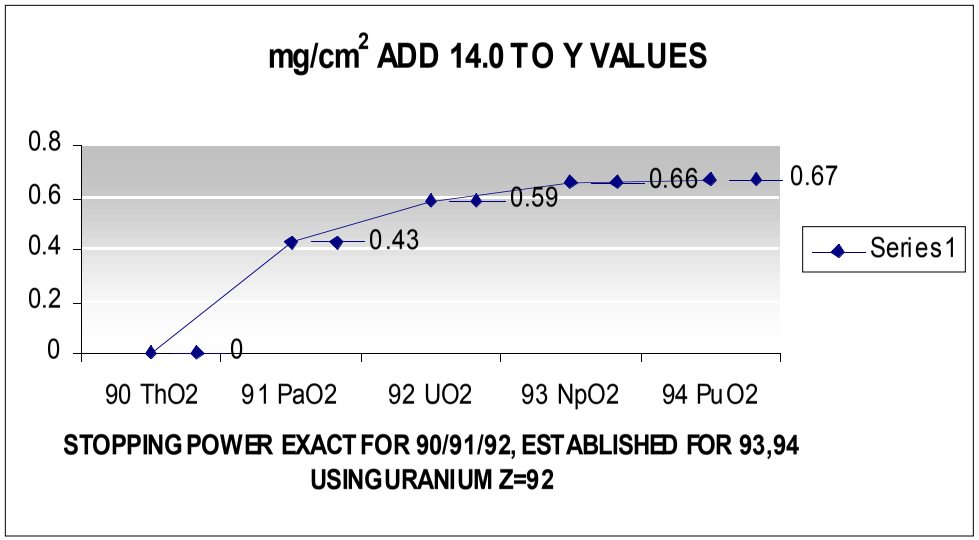

Fig. C-1.

Los Alamos
NATIONAL LABORATORY
Los Alamos, New Mexico 87545